GUIDEBOOK FOR 2021 CORDILLERAN SECTION OF GSA FIELD TRIP

HYPOGENIC KARST OF THE GREAT BASIN

Louise D. Hose

Department of Geological Sciences and Engineering, University of Nevada, Reno, NV 89557, USA; hose@drkarst.net

Harvey R. DuChene

Karst Waters Institute, PO Box 362, Lake City, CO 81235 USA; hrduchene@gmail.com

Daniel Jones

Department of Earth and Environmental Science, New Mexico Institute of Mining and Technology, Socorro, NM, 87801 *USA; National Cave and Karst Research Institute, Carlsbad, NM, USA*

Gretchen M. Baker

Great Basin National Park, Baker, NV 89311, USA; Gretchen_Baker@nps.gov

Zoë Havlena

Department of Earth and Environmental Science, New Mexico Institute of Mining and Technology, Socorro, NM, 87801 *USA*

Donald Sweetkind

U.S. Geological Survey, Denver, CO, USA

Doug Powell

Humboldt-Toiyabe National Forest, Ely Ranger District, Ely, Nevada, 89301, USA

ABSTRACT

Discoveries in the 1980s greatly expanded speleologists' understanding of the role that hypogenic groundwater flow can play developing caves at depth. Ascending groundwater charged with carbon dioxide and, especially, hydrogen sulfide, can readily dissolve carbonate bedrock just below and above the water table. Sulfuric acid speleogenesis, in which anoxic, rising, sulfidic groundwater mixes with oxygenated cave atmosphere to form aggressive sulfuric acid (H_2SO_4), formed spectacular caves in Carlsbad Caverns National Park. Cueva de Villa Luz in Mexico provides an aggressively active example of sulfuric acid speleogenesis processes, and the Frasassi Caves in Italy preserve the results of sulfuric acid speleogenesis in its upper levels while sulfidic groundwater currently enlarges cave passages in the lower levels.

Many caves in east-central Nevada and western Utah are products of hypogenic speleogenesis and formed before the current topography fully developed. Wet climate during the late Neogene and Pleistocene brought extensive meteoric infiltration into the caves and calcite speleothems (e.g., stalactites, stalagmites, shields) coat the walls and floors of the caves, concealing evidence of the earlier hypogenic stage. However, by studying the speleogenetic features in well-established sulfuric acid speleogenesis caves, evidence of hypogenic, probably sulfidic, speleogenesis in many Great Basin caves can be teased out. Compelling evidence of hypogenic speleogenesis in these caves include folia, mammillaries, bubble trails, cupolas, and metatyuyamunite. Sulfuric acid speleogenesis signs include hollow coralloid stalagmites, trays, gypsum crust, pseudoscallops, rills, and acid pool notches. Lehman Caves is particularly informative as a low-permeability capstone protected about half of the cave from significant meteoric infiltration, preserving early speleogenetic features.

INTRODUCTION

Geologists have long wondered about the origins of many dry caves and solution pockets in east-central Nevada. These caves have neither stream deposits nor other evidence of previously flowing water. Their ceilings commonly have small domes (often called cupolas), blunt bedrock pendants that resemble giant bones, ("boneyard," as described by White, 1988), and passages that abruptly end. Unusual speleothems (secondary cave deposits), like mammillaries and folia, also puzzled early explorers. Speleologists traditionally called these sites "phreatic caves" (caves formed in the saturated zone or aquifer), but wondered how they formed below the water table and now rest high in desert mountains.

Discoveries in the 1980s greatly expanded speleologists' understanding of how caves like these formed, especially with recognition of the role of hypogenic groundwater flow. Understanding grew about the process of sulfuric acid speleogenesis in which anoxic, sulfidic groundwater mixes with oxygenated cave atmosphere to form aggressive sulfuric acid (H_2SO_4) (Palmer, 2013). Perhaps most revolutionary was the acknowledgment that microbes greatly facilitated and mediated many speleogenetic processes. Leading the charge in changing our understanding of these type of caves were the groups working on Movile Cave in Romania (Sarbu et al., 1996), the Frasassi Caves in Italy (Galdenzi and Jones, 2017), Guadalupe Mountain caves in New Mexico (DuChene et al., 2017), and Villa Luz cave in Mexico (Hose et al., 2000). The much-less studied Lehman Caves (a single, multi-room cave) in Great Basin National Park and other Great Basin caves contain features that are strongly suggestive of sulfuric acid speleogenesis.

On this field trip, we take advantage of the virtual format to "visit" four distinctly different locations. Many of these sites are only accessible by technical caving, which would not be possible in a traditional field trip format. The first part of the trip focuses on four well-

established, hypogenic, sulfuric acid speleogenesis caves: Cueva de Villa Luz in Mexico, the Frasassi Caves in Italy, and Carlsbad Cavern and Lechuguilla Cave in the Guadalupe Mountain of New Mexico. As we tour these sites, we will focus on features that are similar to those in Lehman Caves to provide background information prior to our visit to east-central Nevada.

We start our tour in southern Mexico at the aggressively active, sulfidic, hypogenic Cueva de Villa Luz (Fig. 1). Recognized for centuries by the indigenous people as a spiritual place, Villa Luz received notoriety in the late 1990s when U.S. scientists began studying its robust, chemoautotrophic-based ecosystem and rapid speleogenesis. We will use this stop to observe active sulfuric acid speleogenesis and its products.

Our second stop is at a commercial cave in east-central Italy, Grotte di Frasassi (Fig. 2). This remarkable cave displays both active sulfuric acid speleogenesis and its relict products. The lower parts of the cave are undergoing active cave development. Today, upper passages are well above the sulfidic water table and resemble the Guadalupe Mountain caves (Stops 3 & 4) with abundant calcite speleothems as well as remnants of sulfuric acid speleogenesis.

Our next two stops will be in the Guadalupe Mountains in New Mexico, USA, focusing on two large caves in Carlsbad Caverns National Park (Fig. 3). First, we visit Carlsbad Cavern where observations and research on sulfuric acid speleogenesis started in the early 1970s (Egemeier, 1971; Davis, 1973; Hill, 1987) and continue today. Carlsbad is an outstanding and accessible location for viewing evidence of ancient sulfuric acid speleogenesis. Our fourth stop is Lechuguilla Cave where all of the sulfuric acid speleogenesis-related features of Carlsbad Cavern are preserved in exquisite, undisturbed detail.

The second part of the trip moves to east-central Nevada and starts with an overview of the regional geology from Stop 5 at Sacramento Pass, which divides the northern and southern Snake Range (Fig. 4). Both parts of the Range are underlain primarily by Late Proterozoic to Permian strata; however, multiple deformational episodes, including the development of the Snake Range décollement in Miocene time, have modified Paleozoic strata and greatly disrupted the continuity of the carbonate-rock section.

Stop 6, Lehman Caves in Great Basin National Park, provides the overall focus and inspiration for this field trip. Lehman, a show cave, has been regularly visited since 1885 and serves as one of the main attractions at the park. Yet, only very limited geologic studies had been made before 2017. We will look at evidence in the cave that supports the hypothesis of a hypogenic, sulfuric acid speleogenesis origin.

The remaining stops will include visits to other caves in the region that display evidence of hypogenic, perhaps sulfidic, speleogenesis (Fig. 4).

STOP 1. CUEVA DE VILLA LUZ, TABASCO, MEXICO

Cueva de Villa Luz near Tapijulapa, Tabasco, Mexico, is a splendid example of an active, sulfidic, hypogenic cave. A stream flows over the floor of approximately two kilometers of braided passage (Fig. 5). At least 26 sulfidic, thermal springs rise from the floor, many of which are anoxic (Hose et al., 2000). Water temperature is 28ºC, roughly 2ºC higher than the ambient outside and the cave-wall temperatures. The most sulfidic of the springs have H_2S content of 300-500 mg/L, no measurable O_2, PCO_2 = 0.03-0.1 atm, and pH ranging from 6.3 to 6.9 (Hose et al., 2000).

Sulfide gas in the cave atmosphere varies temporally and with location. Our team carries personal gas monitors (O_2, H_2S, CO, and CH_4 or CO_2), face masks with appropriate filters, and, in areas known for particularly toxic air, small SCUBA bottles. We also wear knee-shin pads, helmets, and headlamps with backup lights readily available.

One of the most striking features of the cave is the robust ecosystem. Abundant microbial colonies utilize reduced sulfur and other chemical nutrients to form the base of the food chain. Invertebrates consume the microorganisms, other invertebrates, and even small vertebrates. Small fish that live in the stream also eat the microbial biofilms and midges.

Geologic Setting

Cueva de Villa Luz sits at 79-m asl within a middle Cretaceous limestone in the Sierra de Chiapas foothills. The region has a complex tectonic history including extensional faulting in Late Triassic and Jurassic times with the opening of Gulf of Mexico. Minor uplift began in the Late Cretaceous and compression and transpression caused folding and left-lateral strike-slip and thrust faulting (Hose and Rosales-Lagarde, 2017). In the Neogene, a northwest-trending fold belt developed. Rosales-Lagarde et al. (2014) determined, based on isotopic composition, that water flowing into Cueva de Villa Luz mostly derives from meteoric water infiltrating in the Sierra highlands that then follows deep, long flow paths through anhydrite layers interbedded in underlying, Early Cretaceous and Late Jurassic carbonate units.

Location and Route to Cave

Cueva de Villa Luz is part of the Villa Luz Regional Park about two kilometers south of the village of Tapijulapa, Tabasco, Mexico (Fig. 1). It may be easily accessed by foot or a

combination of small boat travel up the Oxolotán River from Tapijulapa followed by a one-kilometer walk. Requirements for permission to enter the cave change frequently so check with local officials before a visit. Kolem Jaá (http://kolemjaa.com/), a nearby rustic hotel and adventure tourism center, may be able to facilitate a visit to Villa Luz.

Stop 1.1. Main Entrance Room

Cueva de Villa Luz has been a site of an annual indigenous ceremony based on the abundance of mollies (*Poecilia mexicana*) living in the cave stream. A platform, stands, and cement steps leading into the cave were built for this ceremony, which brings hundreds of people to the cave on Palm Sunday.

You will immediately be aware of the hydrogen sulfide odor as you approach the cave. In the first room, the H_2S levels are typically below 10 ppm. However, as you travel upstream, H_2S concentration generally increases and occasional "bursts" near springs have been observed to exceed 210 ppm, the limit of our monitoring equipment. It is time to don a gas mask and turn on the gas monitor.

Although parts of the cave are highly acidic, the stream and the muck on its floor have circum-neutral pH values of 6.4-7.2. If the muck (an organic-rich mixture of insoluble sand grains, tiny snail shells, and microbes) remains trapped between your kneepad (or elsewhere) and skin, be sure to occasionally rinse and remove it. You'll be thankful for the mask as it also filters out the clouds of midges that fill the air and are part of the robust ecosystem. Midges consume the abundant microorganisms and provide a significant part of the mollies' diet, with microbial biomass making up the remainder.

As we wade, and crawl for a short stretch, through the stream, careful observers will note water rising from dozens of cracks and holes in the floor (Fig.5). This water is clear but sulfidic. However, the main stream is cloudy and white due to suspended sulfur and microbial filaments (Hose et al., 2000; Rosales-Lagarde, 2013). You will often not be able to see where you are stepping, making the shin pads priceless.

The cave has many skylights (Fig. 5), probably the sources of its name, *Villa Luz (Lighted Home)*. Most skylights are immediately above or just downstream from sulfidic springs in the cave. Cupolas, small smooth-wall domes without obvious fissures cross-cutting them, are located above other springs. These ceiling features result from sub-aerial dissolution concentrated above the sulfide-releasing springs.

Stop 1.2. Sala Grande Area

We start our Sala Grande visit by crawling into a nearby side passage where we will experience the cave's highest sulfide concentrations in the Yellow Roses room. A highly sulfidic, anoxic spring rises from the floor in this small room which has a very high ceiling. The pH of the spring has been measured as low as 6.3, and H_2S concentrations range from 300-500 mg/L with varying small amounts of formaldehyde (Hose et al., 2000). Air measurements in this room have shown maximum H_2S concentrations above 210 ppm (monitor's upper limit) and minimum O_2 below 9%. The most remarkable features here are the sulfur folia and botryoidal sulfur deposits on the walls (Fig.6).

Folia, most commonly calcite but also reported as mud and halite, have been identified in about 30 caves worldwide (D'Angeli et al., 2015. Their origin is unclear and controversial (Audra *et al*., 2009; Davis, 2012) but they are most often associated with hypogenic caves and thought to

form at or just below a fluctuating water level. Villa Luz's folia and botryoidal sulfur are clearly subaerial, above the high-water level (Fig. 7), and made up of elemental sulfur and abundant microbes. These folia grow on selenite needles and, due to inadvertent breakage of some folia and underlying selenite, we know that they can re-generate in about 10 years. This observation supports Davis' (2012) theory of accretion and adds the intriguing idea that the morphology of these sulfur folia (and perhaps other forms?) is controlled by microbial activity.

In the main Sala Grande, we see many of the processes relevant to our upcoming visit to ancient, sulfidic caves. Several small, thermal springs rise from vents that release H_2S and water vapor from the springs. The vapor condenses on the cooler walls, mixes with oxygen from the surface, and, greatly facilitated by sulfur oxidizing microorganisms, forms sulfuric acid. Villa Luz's most famous feature are the pendulant colonies of bacteria and archaea ("snottites") performing this function, (Fig. 8; Hose and Pisarowicz, 1999). These charismatic microbial colonies are ephemeral, visually changing overnight. Microbially facilitated oxidation of H_2S occurs as follows:

$$H_2S + 2O_2 \rightarrow H_2SO_4 \quad (1)$$

The acid produced by these and other sulfur-oxidizing microbes reacts with the limestone cave walls to form gypsum as either a microcrystalline paste or selenite form. Hence, the walls throughout the cave are mostly covered with gypsum.

$$CaCO_3 + 2H^+ + SO_4^{2-} + H_2O \rightarrow CaSO_4 \bullet 2H_2O + CO_2(aq) \quad (2)$$

The gypsum paste's pH typically ranges from 0.0-3.5. Rich in microbes and water, its low competency and high fluid content keep it from adhering long to the walls and ceiling. Consequently, blobs of gypsum paste slough off the walls and ceilings to fall into the stream,

onto the floor, or on some hapless explorer. Blobs that fall into the stream rapidly dissolve and wash out of the cave. Blobs falling onto dry floor build up as deposits of mushy gypsum sediment, best demonstrated by the slope at the southwest end of Sala Grande (Fig. 9). Workers in ancient, sulfuric acid speleogenesis caves refer to the lithified products of these massive gypsum deposits as speleogenetic gypsum or "glaciers". Gypsum paste blobs falling onto explorers, like drops of snottite acid, can cause chemical burns, especially if landing in one's eye!

The gypsum bank at the southwest end of the room is at least two meters thick. Water dripping from the ceiling has drilled vertical holes into the soft, soluble gypsum. The larger holes and the edges of the bank have rill-like vertical grooves. This actively forming gypsum bank strongly resembles the lithified gypsum deposits in ancient, sulfide-rich, hypogenic caves such as Frasassi (Stop 2), Carlsbad (Stop 3), and Lechuguilla (Stop 4).

Stop 1.3. Pool Room

Moving towards the Main Entrance, we pause at the Pool Room (Fig. 10). The site is an active example of an "acid pool." The pool depth ranges from one to one-and-a-half meters with muck covering the floor. The walls and ceiling above the pool are coated with gypsum paste and occasional snottites. On the ceiling, concave pockets filled with gypsum paste are separated by downward-protruding pendants that commonly have a dense cover of small gypsum crystals at their tips. The crystals coat the underlying bedrock, shielding it from acid and locally preventing the acid from reacting with the limestone. Liquid drops hanging from the gypsum are highly concentrated sulfuric acid. The concave pockets between the pendants range from a few centimeters to more than a meter across and are not consistent in size. The bedrock shelves along the edge of the pool have deeply carved rills that resulted from strongly acidic condensation

water flowing down, under the gypsum paste, onto the shelf and into the stream (Fig. 11). Rills are also likely forming under the gypsum paste higher on the walls.

After bedrock is exposed either by sloughing of gypsum paste or dissolution by freshwater infiltration, microbes colonize the exposed limestone (Fig. 12). This process is rapid and month-to-month changes are observable. The brown, purple, red, and dark gray bacteria clusters (biovermiculations) have typical pH values of 3.1 to 3.8. They appear to serve as pioneer colonies on exposed bedrock surfaces.

The highly acidic environment within the gypsum paste and biovermiculations dissolves shallow, concave pockets into the bedrock. In ancient sulfidic, hypogenic caves like Carlsbad and Lechuguilla, we commonly see walls covered by shallow pockets that superficially resemble cave scallops as described and explained by Rane Curl (1974) to determine direction and velocity of water flow. However, the apparent scallops in the Guadalupe and Lehman caves do not demonstrate the consistent size and asymmetry of scallops that form on limestone in a flowing water environment. We believe the "scallops" in ancient sulfidic, hypogenic caves result from uneven dissolution beneath gypsum paste and clusters of biovermiculations. Although we have not observed the texture under Villa Luz's active gypsum paste, where we can see the underlying bedrock, the texture is uneven and consistent with the development of "pseudoscallops."

Other notable features at this pool are the wall indentations just above current, baseline stream level. These notches likely formed initially when the pool was a few centimeters higher and represent a mixing zone where highly acidic condensate moisture flowing down the wall from under the gypsum paste merges with the stream water.

Today, in this room, these notches represent the current height of flood events when meteoric water enters the cave following very large rain events (e.g., hurricanes). The acidic gypsum paste falls onto the shelves in between storms. Acidic condensate flows under the gypsum and etches the floor rills. When the stream rises, the gypsum is washed away and the bedrock with rills is exposed.

STOP 2. FRASASSI CAVES, MARCHE REGION, ITALY

The Frasassi Caves make up a spectacular cave system in Italy's Marche region (Fig. 2). The caves are among the most popular show caves in Italy (Garofano and Govoni, 2012), and are world renowned for their impressively large chambers and beautiful ornamentation. To the speleological community, however, Frasassi is known as an exceptional system for studying sulfuric acid speleogenesis. Relict features from ancient sulfuric acid corrosion in the upper-level show cave can be traced to active sulfidic processes that are occurring today in the lowermost levels.

For this tour, we will start in the sulfidic lower levels and work our way up to the older levels. This will allow us to observe the transition from an active sulfidic cave to a "fossil" sulfidic system, in which many of the features associated with sulfuric acid speleogenesis have been overprinted by epigenic processes.

Geologic Setting

The caves are located in the Frasassi Gorge (N 43°24′ E12°57′), a steep-walled canyon cut by the Sentino River near the towns of Genga and San Vittore, roughly 40 km from the Adriatic Sea (Fig. 13). The gorge is incised through the Mt. Frasassi-Mt. Valmontagnana anticline, part of the

northeast-central Apennines fold-and-thrust belt. Most of the cave is developed in the Jurassic Calcare Massicio formation, a massive platform limestone that is roughly 1000 m thick.

The largest cave is the Grotta Grande del Vento-Grotta del Fiume (GGV-GdF) complex, although there are many other caves in the immediate area. The GGV-GdF includes the show cave portion, as well as the lower levels that encounter the sulfide-rich aquifer. Sulfidic groundwaters emerge as anoxic or micro-oxic springs and lakes, with dissolved sulfide concentrations up to 600 μM. The lowest known level is submerged, and contains substantial underwater passages that are still being explored (Montanari et al., 2019; Macalady et al., 2019). Readers are referred to Galdenzi and Maruoka (2003), Mariani et al. (2007), and Montanari et al. (2019) for more detailed geologic information.

Two of the other largest caves in the area are the Buco Cattivo, which lies directly atop the GGV-GdF system, and the Grotta del Mezzogiorno-Grotta di Frasassi (GM-GF) on the northern side of the gorge. These two caves are 150-300 m above the current water table. No connection between Buco Cattivo and GGV-GdF is currently known, although one may exist (Mariani et al., 2007).

Location and Route to Cave

The show cave portion of the GGV-GdF (the GGV) is accessed through an artificial tunnel. Visitors can park and purchase tickets two kilometers away at the “parcheggio e biglietteria” (N43.403253^{o}, E12.976392^{o}), and either take a bus or walk to the cave entrance. The GGV-GDF can also be accessed through a few smaller entrances with appropriate permissions.

Stop 2.1. Cave Springs and Sentino River

Along the road from the ticket office to the cave entrance, visitors have the opportunity to see and smell the sulfidic groundwaters that are responsible for the formation of the cave. A few sulfide-rich springs emerge into the Sentino River, which can be accessed by a path along the river.

Springs can be located by their characteristic white color, which is created by white mats of sulfide-oxidizing microorganisms. The whiteness comes from biogenic elemental sulfur that accumulates in the mats and inside the cells of filamentous sulfide-oxidizing bacteria. In fast-flowing waters, these mats (or biofilms) usually have a feathery morphology and are known as "streamers," which attach to the substrate and are sometimes large enough to "flap" in the current. In more stagnant areas, the mats form at the sediment-water interface where the microbes that form them can move vertically in the sediment (Macalady et al., 2008). In some places, the white mats are associated with green and even pink mats, which are formed by cyanobacteria and anoxygenic phototrophic bacteria (Klatt et al., 2016).

The largest emergence is known as the Cave Springs, which has saline, microoxic waters with typically 100-300 μM dissolved sulfide and 5-15 μM dissolved oxygen (Macalady et al., 2008; Jones et al., 2015). The spring waters are slightly salty and circumneutral, with conductivity values between 1500-2500 μS cm^{-1} and pH between 7.1-7.3. Some springs in the area such as "Fissure Spring" are consistently more saline, with conductivities in the range of 2500-3500 μS cm^{-1}, 350-600 μM sulfide, and <5 μM dissolved oxygen. These more concentrated waters have experienced little to no mixing with fresh waters on their path to the surface (Galdenzi et al., 2008). Sulfidic springs and lakes inside the cave have similar water chemistries to these springs.

Stop 2.2 Pozzo dei Cristalli

The next stop is inside the cave. The sulfidic aquifer is accessible in Pozzo dei Cristalli at the bottom of an 18-m pit. Here, several springs bring deep-seated sulfidic waters into contact with the oxygenated cave atmosphere, one of which forms a stream that flows for several meters before resubmerging. At this site, one can observe many of the features associated with active sulfuric acid speleogenesis that were described in Stop 1, Cueva de Villa Luz.

Like the springs outside the cave (Stop 2.1), white microbial mats fill the stream and usually coat every available sediment surface (Fig. 14a). The morphology of the mats, which corresponds to the dominant population of sulfide-oxidizing bacteria, varies depending on the sulfide-oxygen ratio and the turbulence of the stream. Under very slowly flowing conditions, the stream is filled with veil-like films produced by *Thiovulum* spp. (Macalady et al., 2019), which change to *Beggiatoa*-dominated mats that form at the sediment water interface, and eventually to streamers created by *Epsilonproteobacteria* (or *Thiothrix* in other cave locations) as streams become more turbulent and the oxygen influx increases (Macalady et al., 2008). Endemic invertebrates thrive in the stream and feed off the biomass from the chemosynthetic mats (Galdenzi and Sarbu, 2000). An abundant amphipod that is found throughout the cave, *Niphargus ictus*, was even discovered to have a symbiotic relationship with sulfide-oxidizing bacteria (Dattagupta et al., 2009).

Sulfide degassing creates a substantial sulfide flux to the cave atmosphere, especially when streams are fast flowing and turbulent (Jones et al., 2015). On the trail to the pit, visitors begin to notice microcrystalline gypsum wall crusts and a strong H_2S smell, which increases during the descent into the pit. Small snottites can be observed in some places where gypsum crusts overhang the stream, but are not common at Pozzo dei Cristalli, likely because the open pit

allows hydrogen sulfide gas to quickly diffuse such that concentrations remain low. Biovermiculations at this and many other sites in Frasassi are impressive and cover large swaths of limestone wall, especially at the top of the pit and in areas more distal from the stream, although they can also be observed near the stream where patches of limestone peek through the gypsum crust (Fig. 14b). The distribution of microbial features generally follows that depicted in Figure 15, with snottites near the actively degassing streams and biovermiculations farther away in areas where gypsum crusts thin and give way to exposed limestone.

At this location, we can also observe remnants of older sulfidic stream channels that were created when the water table was slightly higher than at present. These older stream channels have phreatic conduits created by rising sulfidic waters, dissolution notches carved at the air-water interface (like that of the acid pools in Villa Luz), and sometimes, keyhole morphologies with overhead cupolas.

Stop 2.3. Ramo Sulfureo

The next stop is another site at the sulfidic water table, which is deeper inside the cave and requires a longer and muddier trip. Sulfidic waters are exposed at several locations in the Ramo Sulfureo (Sulfurous Branch). Hydrogen sulfide gas concentrations are higher here, exceeding 20 parts per million by volume (ppmv) in some more enclosed spaces. In these areas with high sulfide gas concentrations, the walls have abundant snottites and, in some places, small elemental sulfur deposits. Snottites in Frasassi are much smaller than in Villa Luz, although like Villa Luz, Frasassi snottites are extremely acidic (pH 0-1) and are colonized by similar groups of extreme acidophilic bacteria and archaea (Jones et al., 2016; D'Auria et al., 2018).

Stop 2.4. Abisso Ancona and Sala della Sabbia in the Show Cave

We now travel from the sulfidic water table up to some of the older levels in the show cave that are approximately 30-40 meters above the present water table. Because the northeast-central Appenines that host Frasassi are slowing rising, the higher cave levels have been progressively removed from the water table (Mariani et al., 2007; Montanari et al., 2019). In these upper levels, carbonate-saturated surface waters have taken over and created the beautiful decorations and impressive speleothems that are part of Frasassi's allure as a show cave. While these more recent epigenic processes have overprinted many of the pre-existing hypogenic features, evidence of the cave's sulfidic past can be found in isolated patches of gypsum and in various characteristic morphologies (Galdenzi and Jones, 2017).

The Abisso Ancona in GGV is one of the largest cave chambers in Europe, with an impressive volume of roughly 10^6 m^3 (Galdenzi and Maruoka, 2003) and large enough to comfortably contain the Milan Cathedral. The natural entrance that led to the discovery of GGV in 1971 sits above the Abisso Ancona, and early explorers accessed the cave by dropping down long cable ladders to the bottom of the massive chamber. Several large gypsum "glaciers" can be seen from the tour trail, including some smaller deposits high above. These deposits have light isotopic compositions ($\delta^{34}S_{sulfate}$ between -8 and -16‰), consistent with their formation by degassing H_2S (Galdenzi and Maroka, 2003). These ancient gypsum deposits persist where they are protected from infiltrating fresh waters, and commonly have drip holes and grooves created by gypsum-undersaturated surface waters.

Further along the tour trail, a large gypsum deposit can be seen off in the distance in Sala della Sabbia (Fig. 16). The deposit has a white gypsum upper layer and a grey gypsum-clay lower portion, and sits atop the only known sand deposit in the cave. This sand was recently dated

using luminescence methods with a burial age of 129–101 ka, which helps constrain the formation of the passage and the tectonic uplift rate of the region (Montanari et al., 2019).

Stop 2.5. Artificial Sulfidic Spring Along the Tourist Trail

Other than visiting the springs in the Sentino River (Stop 2.1), visitors to the show cave in the past did not have an opportunity to see and smell the sulfidic action that is responsible for the cave's splendor and its hidden chemosynthetic ecosystem. Now, however, the tour passes by aquariums that contain *Niphargus* and other invertebrates from the sulfidic levels, as well as a small artificial spring. The spring is fed by water pumped from a stratified sulfidic lake (Lago del Orsa), and flows for a few meters over a limestone channel. Since it was established in 2012, the spring has organically developed into a microcosm of the lower cave levels, with white microbial mats, microcrystalline gypsum, patches of biovermiculations, and even small snottites. Work is ongoing to determine the genetic relationships between the microbiota of the artificial spring and that of the lower levels.

Stop 2.6. Entrance to Grotta del Mezzogiorno-Grotta di Frasassi (GM-GF)

The last stop is a brief visit to some even older levels that represent a much earlier stage in the evolution of the Frasassi Caves. The GM-GF is a 3500-m long cave on the north side of the Sentino River, more than 150 meters above the current water table. A long staircase leads to the cave, which has a small church built in the entrance alcove (sometimes known as Grotta della Madonna). These older levels probably formed in a different geologic and hydrologic setting than the GGV-GdF complex, with only rare features that could be attributable to subaerial sulfuric acid corrosion (Galdenzi and Jones, 2017). The age of these older levels can be

constrained by cosmogenic dating of fluvial sand near the entrance of GM-GF, which provided a burial age of 0.75 ± 0.26 Ma (Cyr and Granger, 2008).

STOP 3 AND 4. GUADALUPE MOUNTAINS, NEW MEXICO

Carlsbad Cavern and other caves in the Guadalupe Mountains were studied in the early 1970s by Egemeier (1971, 1987), Davis (1973; 1980) and Jagnow (1977), all of whom recognized that sulfuric acid played a role in speleogenesis. Concurrently, Hill (1987) began a study of the mineralogy of Carlsbad, and as part of her project, discovered that sulfur in the massive gypsum deposits in the cave is isotopically light ($\delta^{34}S$ = -13.9‰). For many years, the gypsum in the cave was thought to have been dissolved from the evaporites in the Castile Formation in the nearby Delaware basin, in which the sulfur is isotopically heavier ($\delta^{34}S$ = +10.3‰, avg.). Hill recognized from the isotopic study that the gypsum in Carlsbad could not have come from the Castile Formation but had to originate from hydrocarbons, and she immediately changed the focus of her studies from mineralogy to speleogenesis. She collected data and described features in Carlsbad Cavern for almost 10 years, then published her work in a monograph entitled *Geology of Carlsbad Caverns and Other Caves in the Guadalupe Mountains, New Mexico and Texas* (Hill, 1987). More recently, Arthur and Margaret Palmer have clarified the processes of sulfuric acid speleogenesis in numerous publications (e.g., Palmer and Palmer, 2000, 2012; Palmer, 2007, 2013).

Carlsbad Cavern has 63 km of passage and is 315 m deep. Mineralogic, speleogenetic and speleothemic features that characterize sulfuric acid speleogenesis caves are exposed throughout the cave although some have been impacted by use and development for tourism. However, the cave remains an outstanding and accessible location for viewing evidence of sulfuric acid

speleogenesis, and many features can be seen along the tourist trail through the entrance passage and around the Big Room.

Lechuguilla Cave was discovered in 1987, although the entrance was known much earlier. Lechuguilla has >248 km of known passage, is 488 m deep, and contains all of the features of Carlsbad Cavern preserved in exquisite, undisturbed detail.

During our virtual tour through Carlsbad Cavern and Lechuguilla Cave, we will examine evidence of sulfuric acid speleogenesis. Most of the Carlsbad Cavern features are in the visitor-accessible Big Room and Left-Hand Tunnel. The features in Lechuguilla are only accessible to qualified exploration and science teams with permission of Carlsbad Caverns National Park.

Geologic Setting

The Guadalupe Mountains rise westward above the high plains of southeast New Mexico to a magnificent culmination at Guadalupe Peak in west Texas (Fig. 3). The Guadalupes are part of the Capitan Reef, a feature that rimmed a Permian sea in this region approximately 273 - 260 Ma (Hayes, 1964; Cohen et al., 2013). The reef borders the Delaware Basin, a rich source of hydrocarbons. In the basin center, hydrocarbon-bearing strata are capped by evaporite beds that contain H_2S and deposits of sulfur. Most hydrocarbon accumulations in Guadalupian strata north of and adjacent to the Capitan shelf margin contain H_2S. These accumulations, or the H_2S in Ochoan evaporites, are probable sources of the sulfuric acid that drove sulfuric acid speleogenesis in the Guadalupe Mountains.

Epeirogenic uplift of the southern Rocky Mountains may have begun as early as 38 Ma ago (Eaton, 2008) and ultimately resulted in crustal extension and the development of the Rio Grande Rift. The uplift elevated western and central New Mexico and west Texas, causing crustal

extension and erosion that exposed the northwestern part of the Capitan Reef Complex. The exposed limestone and dolomite of the reef was carved and sculpted into a labyrinth of deep, rugged canyons and ridges where hundreds of caves are hidden (DuChene and Martinez, 2000). Uplift created a strong, eastward-directed confined hydrodynamic flow system that introduced meteoric water into the Capitan aquifer (DuChene and Cunningham, 2006). Around 12 Ma, the water table began to fall in response to regional tectonic extension and erosional downcutting (Polyak et al., 1998). Sulfuric acid speleogenesis occurred at or just above the water table, significantly enlarging older, fracture-controlled cave passages. H_2S that caused sulfuric acid speleogenesis reached the water table by migrating upward through steeply inclined fracture-controlled passages. Today, the water table is beneath all of the known caves in the Guadalupe Mountains, except Lechuguilla, and reaches the surface at Carlsbad Springs near the city of Carlsbad.

Location and Route to Carlsbad Caverns National Park

Carlsbad Caverns National Park is in southeast New Mexico, 58 km north of the Texas state line (Fig. 3). The entrance to the Park is 33 km southwest of the City of Carlsbad and 233 km east of El Paso. Access to the Park is at Whites City where the entrance road intersects US Highway 180-W/US 62-W. The Visitor Center, where entry tickets can be purchased, is at the end of a 12-km drive through Walnut Canyon. The distance from the cave entrance to the Big Room is two kilometers to where it joins with a two-kilometer trail around the Big Room. The trail in the Big Room can also be accessed by an elevator from the Visitor Center.

Stop 3. Carlsbad Cavern

Stop 3.1. Entrance to Carlsbad Cavern

Access to Carlsbad Cavern is through one of the most spectacular entrances in the Guadalupe Mountains. The field trip route follows the tourist trail through the Entrance Passage to its intersection with trails around and through the Big Room. The impressive entrance passage ranges up to 50-m wide and high and descends 243 m to the Big Room. All of our stops are in the Big Room and Left-Hand Tunnel (Fig. 17).

Stop 3.2. Trays on Wall Next to Tourist Trail, Big Room

As we enter the Big Room, notice that the nearby wall of the cave on the right is covered with trays, which are flat-bottomed speleothems composed of botryoidal calcite and aragonite (Fig. 18). Note that the bottoms of the trays are flat but not necessarily horizontal or parallel to each other. They occur at multiple levels on the wall, and the basal planes have various attitudes ranging from horizontal to slopes of a few degrees.

Trays were first documented in Cango III Cave and Thabazimbi Mine Cave in South Africa by Martini (1986a, b) who described them as "…a speleothem type composed of spray or clusters of popcorn or grape coralloids and frostwork, the composite mass of which ends in a flat horizontal, tray-like surface. Often these flat-bottomed masses occur in tiers or ledges; that is, at different levels along a cave wall, in a stair-step-like manner."

Elsewhere in Carlsbad Cavern, trays are found suspended from low points on passage ceilings, Martini (1986b, p. 2-3) noted that "Their peculiar character [of trays] is due to the fact that they develop only horizontally and vertically but cannot grow downward, as if in this direction they are limited by some invisible barrier. Observations show that this limit does not correspond to a

former surface of a pool, as the "trays" develop at any level & that their positions are controlled by the elevation of the roof pendant extremity. It was also observed that water is actively dripping from the "trays" and is saturated or slightly undersaturated in calcium carbonate as no deposition occurs on the floor below the trays: on the contrary, corrosion holes have been observed in the carbonate crust."

More will be said about trays at Stops 4.8 and 6.6

Stop 3.3. Big Room Near Fairyland

This stop highlights a field of coralloid-encrusted drip tubes and associated early-stage speleothems that formed in and under masses of speleogenetic gypsum (Fig. 19). A hypothesis for their formation is that dripping water bored through the gypsum mass, depositing a case-hardened mineral lining composed of calcite (Fig. 20). The tube remained after the gypsum was dissolved and transported elsewhere. Drip tubes that were not connected to the floor were not preserved, but those that were attached survived. Calcium carbonate-saturated water on the floor of the cave wicked upward into the walls of drip tubes where the carbonate was deposited on the exterior as coralloidal or botryoidal calcite and needles of aragonite. Coralloid-encrusted drip tubes indicate the former presence of massive gypsum and are secondary indicators of sulfuric acid speleogenesis.

Stop 3.4. Tunnel Through Gypsum Mass Near the Jumping Off Place

A few steps from the Jumping Off Place, the trail passes through a tunnel carved into a large mass of speleogenetic gypsum. The tunnel exposed drip tubes which were formed when water from points on the ceiling bored vertical holes through the gypsum (Fig. 21). These holes commonly display vertical fluting and, in some cases, have case-hardened walls. Dripping water

dissolved the gypsum and transported it out of the cave. The Big Room has numerous sites where massive gypsum remains, but this is only a small fraction of the total amount that must have once filled this immense chamber.

Stop 3.5. **Mirror Lake**

On the opposite side of the room from Mirror Lake is an alcove containing a massive gypsum "glacier" formed during the sulfuric acid speleogenesis event (Fig. 22). Breakdown (talus) blocks lie on the floor between the large gypsum mass and the trail. The concave ceiling above and the wall to the right of the gypsum mass are pocked with cuspate concave pseudoscallops that were formed during active sulfuric acid dissolution approximately 3.8 Ma (Polyak et al., 1998). Active sulfuric acid caves have similar features coated with highly acidic gypsum paste (Stops 1.7 and 2.4). Notice that the gypsum mass rests on breakdown blocks similar to those in the foreground, indicating that ceiling collapse preceded the last phase of sulfuric acid speleogenesis. Numerous vertical drip tubes are exposed on the face of the gypsum mass.

Stop 3.6. **Solution Rills Near Left Hand Tunnel, Carlsbad Cavern**

The rills here formed by acid draining from gypsum during sulfuric acid speleogenesis (Fig. 23). Hydrogen sulfide in the cave atmosphere was absorbed into surface water on bedrock where it combined with O_2 and converted to sulfuric acid (H_2SO_4) (Fig.11). The acid reacted with the limestone, forming gypsum paste, which acts like a sponge full of concentrated acid. The pH of the acid is driven down with time as H_2S is absorbed from the atmosphere. As in Cueva de Villa Luz (Stop 1), the paste does not adhere well to the bedrock and sloughs off, falling to the floor or oozing down the wall. Acid drips from low-hanging bedrock pendants or oozes from under

gypsum paste onto sloping bedrock surfaces where it runs downward, dissolving vertical flutes or rills (Palmer and Palmer, 2012).

Stop 3.7. Tyuyamunite

Our last stop in Carlsbad Cavern is Chocolate High, a remote and hard-to-reach area in the uppermost part of the cave. This area lies above the New Mexico Room and was discovered by climbers in 1993 (Doucette, 1993). The area is reached by ascending more than 230 meters of rope in a fissure above the New Mexico Room to a series of passages within limestone and sandstone beds of the Yates Formation. The rare hydrous uranyl vanadate mineral tyuyamunite ($Ca(UO_2)_2V_2O_8$•(5-8)H_2O), or the less-hydrated form, metatyuyamunite ($Ca(UO_2)_2V_2O_8$•3(H_2O)), occurs in sandstone beds of the Yates. Individual crystals are <1 mm, platy, translucent, bright canary yellow and commonly associated with quartz and opal coatings on dolomite, in gypsum crusts and clay deposits. Tyuyamunite and metatyuyamunite are products of U and V precipitation from oxidized groundwater and are associated with and often regarded as supporting evidence for hypogene cave development and possibly sulfuric acid speleogenesis (Polyak and Mosch, 1995; Onac et al., 2001).

Stop 4. Lechuguilla Cave

Location and Route to Lechuguilla Cave

Lechuguilla Cave lies within the Carlsbad Caverns Wilderness Area in Carlsbad Caverns National Park and is not open to the public. The entrance is 6.1 km west-northwest of the Park's Visitor Center and is reached by gravel and two-track, four-wheel drive roads. From the parking area, it is a 1.6 km hike to the entrance. Typical exploration trips last 3 to 6 days, and everything needed for camping underground must fit into a backpack. A visitor to Carlsbad Caverns

National Park once asked “How far can you go into Lechuguilla before you need rope?” The answer? “Well, the first step is 30 meters down.”

And so it is…Lechuguilla has no tourist trail, no artificial lighting, and requires excellent rope and climbing skills. The cave has more than 241 km of mapped passage, is 489 m deep, and has more than 7500 m of fixed ropes (Fig. 24). Its deepest point reaches the water table.

Stop 4.1. Lechuguilla Cave Entrance

The entrance to Lechuguilla is a vertical fissure on a hillside adjacent to Lechuguilla Canyon near the northern boundary of Carlsbad Caverns National Park. The crack was enlarged around 1914 when the cave was mined for its deposits of bat guano, a commodity in demand as a fertilizer. After the cave was dug open in 1986, a culvert was installed to keep breakdown (talus) blocks and dirt from collapsing into the hole. Later, in 2000, the culvert was replaced with a stainless-steel airlock (Richards, 2001). Before the airlock was installed, the cave wind could be heard from 50 to 100 meters away when a low-pressure weather system moved in. Air leaked around the old culvert and made a loud roaring noise and, at times, when the door was open, winds in excess of 120 kph were measured inside the culvert. The wind is an indicator of the tremendous volume of Lechuguilla Cave.

Stop 4.2. Glacier Bay

After negotiating the entrance pit and a 50-m drop at Boulder Falls, we follow a well-worn trail to Glacier Bay, where the first large deposits of speleogenetic gypsum are encountered (Fig. 25). The deposits are 10- to 12-m thick and have been extensively drilled by dripping water. Gypsum has also been dissolved from the bottom of the blocks, causing them to settle and rotate. Several

generations of tubes can be recognized, based on the current orientations of the once vertical tubes.

Massive deposits of gypsum are common in Lechuguilla, occupying large sloping chambers in various parts of the cave. With their white coloration, thickness, and large fragments that calved off the downslope end, they superficially resemble glaciers. All stages of gypsum preservation are represented, ranging from nearly intact deposits to small fragments that remain after the original mass was dissolved by meteoric water. In lower parts of the cave, massive gypsum deposits are mostly absent due to dissolution during a post-sulfuric acid speleogenesis rise in the water table. The range in the degree of preservation helps scientists recognize features that formed during and immediately after the sulfuric acid speleogenesis gypsum deposits dissolved.

The trail continues to a junction with a major cross passage called the Rift, a deep fissure that leads south to the E-F Junction where three major branches of the cave converge. After a short rappel, the route goes through the S&M Crawl, a passage that gets progressively lower until it is only 23-cm high and about 3-m wide. Beyond this low spot, the trail follows a steeply sloping, narrow, and slippery slot canyon to the 30-m climb that leads to Ghost Town, a large room that contains much of the known sulfur in the cave.

Stop 4.3. Ghost Town

Lechuguilla contains abundant evidence of sulfuric acid speleogenesis, but two of the most obvious indicators are many tons of native sulfur and the extensive deposits of massive gypsum. The sulfur in Ghost Town is preserved in passages developed in sandstone beds in the Yates or Seven Rivers Formation. Elsewhere in the cave, native sulfur is partly to mostly encased in

gypsum. Apparently, sulfur in Lechuguilla Cave is preserved only where it is isolated from direct contact with carbonate rocks.

From here we retrace our steps to the top of the Apricot Pit, a continuous 120-m deep series of rope drops leading to The Emperor's Throne Room.

Stop 4.4. **Emperor's Throne Room, Near East**

This large room contains several speleogenetic features ("speleogens") indicative of sulfuric acid speleogenesis. The ceiling and upper wall are deeply corroded by sulfuric acid, leaving an array of ceiling pendants that look distorted and twisted. Just above center in Figure 26 is a horizontal line that formed at the top of an acid pool basin. Below the water line, the wall is much less corroded and is covered by a cream-colored calcite crust covered in part with coralloid speleothems ("popcorn"). The floor is mostly composed of large breakdown blocks that fell from the ceiling during the sulfuric acid speleogenesis event. Most of the features in this room resulted from sulfuric acid dissolution, but may have been later modified by condensation corrosion caused by carbonic acid.

The trail continues east to the Moby Dick Room through both lavishly decorated passages and galleries that are nearly barren. At the east end of this room, a fixed rope extends upward for 67 meters to its anchor point. This is the Aragonitemare, named by the first climbers for the difficulty of the ascent. It leads to the Far East Section of Lechuguilla.

Stop 4.5. Acid Pool Basin, Far East

At this stop in the Bryce Canyon area of the Far East, there is an acid pool basin (see Fig. 11 for explanation) with probable H_2S feeder vent in floor. A water line separates the smooth-walled basin from the corroded margins around the old pool where there are spectacular rills and

spitzkarren. (Fig. 27). Poorly developed pseudoscallops are visible on the ceiling above the kneeling cavers.

When the pool basin was active, this would not have been a pleasant place. The air would have reeked with the odor of rotten eggs and would have been stifling. Based on observations at active sulfuric acid caves, the amount of oxygen in the air was likely low. Some of the drip water was strong sulfuric acid, capable of dissolving rock, and the toxic atmosphere may have been lethal for humans.

After this stop, we retrace our route back to the E-F Junction and then follow the trail that leads to the Southwestern Branch. This route passes through the Chandelier Ballroom and Prickly Ice Cube room to our next stop, a balcony near High Hopes where partially dissolved remnants of massive gypsum blocks lie among coralloid-encrusted drip tubes.

Stop 4.6. **Balcony in Southwestern Branch**

On this balcony, remnants of partly dissolved massive gypsum blocks (Fig. 28) rest adjacent to coralloid-encrusted drip tubes. Partly dissolved fragments of gypsum are scattered across this balcony and there are numerous encrusted drip tubes.

Dissolution of the gypsum occurred after the sulfuric acid speleogenesis event when more meteoric water was available. Gypsum was dissolved, in part, by dripping water and, in part, by condensation water, especially where the masses were in contact with the moist floor. Gypsum was removed at points of contact with the floor causing the block to settle and shift. Drip tubes are vertical when they form, but become tilted when the gypsum blocks settle. A new set of drip tubes formed that cut across the tilted older set. Two sets of drip tubes are visible in the gypsum

mass shown in Figure 28. Some gypsum blocks elsewhere in the cave also show multiple sets of drip tubes (Fig. 25).

Coralloid-encrusted drip tubes are associated with massive gypsum deposits in Lechuguilla. They are steeply conical speleothems attached to the cave floor and are widest at the base and taper upward. The speleothem exteriors are covered with coralloid or botryoidal calcite ("popcorn") and have hollow central tubes. A possible explanation is that the features began as drip tubes through a mass of gypsum. The original drip tube had a hard lining formed either by recrystallization of the gypsum or deposition of calcite. Tubes that were in contact with or cemented to the floor wicked calcium-saturated water upward into the tube by capillarity. Evaporation and/or loss of carbon dioxide caused calcite to precipitate on the exterior of the tube. The wicked water may have been supersaturated with calcium because it contained both dissolved calcium carbonate and calcium sulfate, which resulted in common-ion effect calcite precipitation on the exterior of the drip tube.

Stop 4.7. **Tyuyamunite (or Metatyuyamunite) on Drusy Quartz**

Not far from the balcony, deposits of white drusy quartz are associated with a bright yellow mineral that is either tyuyamunite ($Ca(UO_2)_2V_2O_8$•(5-8)H_2O) or, more likely, the less hydrated variant, metatyuyamunite ($Ca(UO_2)_2V_2O_8$•$3H_2O$). Both minerals belong to the carnotite group of uranyl vanadates and are found in small quantities in Lechuguilla and other Guadalupe caves. Polyak and Provencio (2001) consider tyuyamunite to be a secondary product of sulfuric acid speleogenesis.

Because of its high uranium content, tyuyamunite is radioactive, but it is rare and therefore not a significant ore mineral or health risk. In Lechuguilla and elsewhere, during the era of carbide

lights that produce yellow light, tyuyamunite was frequently overlooked by cave explorers because they could not distinguish the color. When it was seen, concentrations of the tiny bright yellow crystals were often mistakenly identified as sulfur crust.

In Lechuguilla cave, tyuyamunite (or metatyuyamunite) occurs as crusts or as coatings on bedrock walls. It is associated with drusy quartz, opal, calcium carbonate and gypsum crusts (Polyak and Provencio, 2001) and, rarely, with fluorite and celestite.

Our last stop is in Never Never Land, a recently discovered upper-level gallery above the Graveyard Maze in the Western Branch of Lechuguilla. To get there, we retrace our steps by ascending 120 m of rope in Apricot Pit and then drop down the Great White Way to the Western Borehole. From here it is a "relatively easy" horizontal walk to the rope that leads to the Chandelier Graveyard, then up a series of rope climbs to Never Never Land.

Stop 4.8. Never Never Land

Never Never Land was discovered in 2016 in a high area above the Near West section of Lechuguilla. It was found by following a climbing lead above the Western Borehole camp and is mostly developed in the Yates/Seven Rivers Formations (Barton et al., 2020) At the entrance to Never Never Land are several trays underlain by a partially dissolved deposit of speleogenetic gypsum (Fig. 29). Gypsum is not present beneath most of the trays in Lechuguilla, but there are rare sites like this one where they are together. In the center of Figure 29, most of the gypsum has been dissolved by water dripping from the tray, leaving only a few gypsum spires. However, in the upper-right quadrant of the photo, a tray is separated from the underlying gypsum by only one or two centimeters and the slope of the top of the gypsum appears to match the slope of the tray. The close proximity of these trays to speleogenetic gypsum suggests that the flat surface of

the tray could be controlled by the top of the gypsum mass. However, Donald G. Davis (personal communication, 2020) considers the juxtaposition and orientation of the tray and the gypsum mass coincidental.

STOP 5. SACRAMENTO PASS, NEVADA

This field trip stop describes the regional geology of east-central Nevada as an introduction to the second part of the trip at Lehman Caves in Great Basin National Park and other caves in the region. Tilted, fault-block mountain ranges of the eastern Great Basin expose a stratigraphic section of Paleozoic rocks that is predominantly thick-bedded and coarse-grained marine limestone and dolomite; the carbonate-rock section is underlain by Neoproterozoic to lower Cambrian siliciclastic rocks that are only locally exposed (Fig. 30). Where not disturbed by structural complications, this stratigraphic sequence consists of: (1) Neoproterozoic to lower Cambrian siliciclastic rocks that may be 3000-6000 m thick; (2) a Lower Paleozoic section that consists of up to 5000 to 6000 m of middle Cambrian through Devonian predominantly carbonate rocks with relatively thin siliciclastic interbeds; (3) a Mississippian sequence of up to 800 m of mudstone, siltstone, sandstone, and conglomerate and (4) up to 1500 meters of upper Paleozoic carbonate rocks (Kellogg, 1963; Hintze and Davis, 2003). The Paleozoic rocks are unconformably overlain by locally thick Cenozoic volcanic rocks (Best and Christiansen, 1991) and Cenozoic to Recent synorogenic and postorogenic sediments (Grier, 1984).

The Paleozoic carbonate rocks of the eastern Great Basin form a major high-permeability, consolidated-rock aquifer system (Dettinger et al., 1995; Harrill and Prudic, 1998; Heilweil and Brooks, 2011). Permeable carbonate rocks are regionally extensive, form many of the mountain ranges, and underlie the basin-fill and volcanic-rock aquifers beneath many of the valleys in the region. The carbonate-rock, basin-fill and volcanic-rock aquifers are, in some areas,

hydraulically connected between basins (Harrill et al., 1988; Harrill and Prudic, 1998). Groundwater in the carbonate-rock aquifer discharges at perennial-flowing valley-floor springs and, because of the lateral continuity and relatively high permeability of the carbonate rocks, most groundwater flow between adjacent valleys occurs through this aquifer. Based on chemistry, temperature, and other criteria, Mifflin (1968) identified selected springs that likely are discharge points from the regional aquifer system.

The storage and movement of groundwater within carbonate rocks in the eastern Great Basin is governed by the rocks' primary intergranular permeability and secondary fracture or solution permeability. Lower Paleozoic carbonate rocks in southern Nevada have relatively low primary permeability in the rock matrix (Winograd and Thordarson, 1975). Studies of groundwater flow within the eastern Great Basin (Dettinger et al., 1995; Harrill and Prudic, 1998) and tabulations of hydraulic-property estimates for carbonate rocks (Dettinger et al., 1995; Belcher et al., 2001) emphasize the importance of fracture permeability creating a well-connected network of openings through which water can move. Solution openings can create additional secondary permeability in the carbonate rocks (Winograd and Thordarson, 1975). Cook and Corboy (2004) have suggested that solution may occur when shallow marine carbonates are exposed above sea level and are subjected to erosion, dissolution, and development of solution caverns (epigenic speleogenesis). Winograd and Thordarson (1975) proposed that solution permeability may occur locally as solution enhancement of preexisting faults and fractures.

Geologic Setting of the Snake Range and Adjacent Valleys

The Snake Range in east-central Nevada has two distinct topographic culminations that are separated by Sacramento Pass, where Highway 50 crosses the center of the range (Fig. 4). Both the northern and southern Snake Range are underlain primarily by Neoproterozoic to Permian

strata; however, multiple deformational episodes have metamorphosed and deformed some of the rocks and greatly disrupted the continuity of the carbonate-rock section. The consolidated rocks of the Snake Range were intruded by plutons of Jurassic (from 160 to 155 Ma), Cretaceous (from 110 to 90 Ma), and Cenozoic (from 36 to 28 Ma) ages (Lee and Van Loenen, 1971; Lee et al., 1981; Miller et al., 1999).

In the northern Snake Range and the northern half of the southern Snake Range, a gently east-dipping normal fault called the Snake Range décollement separates a lower plate, consisting of granitic rocks and ductilely deformed and metamorphosed Cambrian and Precambrian quartzite, marble, and schist, from an upper plate, consisting of highly faulted, generally unmetamorphosed upper Paleozoic rocks (Miller et al., 1983). The décollement is thought to represent an Oligocene brittle-ductile transition zone (Miller et al., 1983). Geologic and thermochronologic data suggest that the décollement accommodated tens of kilometers of down-to-the-east offset between ca. 37–24 Ma, partly synchronous with regional magmatism and heating, resulting in early, partial uplift of lower plate rocks (Gans et al., 1985; Lee and Sutter, 1991). Local magmatism occurred as part of the "ignimbrite flare-up," an episode of widespread, caldera-forming volcanism that migrated southward across the Great Basin between ca. 43–20 Ma (e.g., Armstrong and Ward, 1991; Brooks et al., 1995), resulting in plutonism and eruption of thick lava flows and tuffs in east-central Nevada during the late Eocene and early Oligocene, ca. 36–32 Ma (Gans et al., 1989; Best and Christiansen, 1991). Eocene–Oligocene motion along the Snake Range décollement was accompanied by extreme extensional thinning of both the upper and lower plates, resulting in a mosaic-like map pattern of fault-bound upper-plate Paleozoic rocks (e.g., Miller et al., 1983; National Park Service, 2007). The magnitude of extension and intensity of

normal fault-related deformation decrease southward in the southern Snake Range as the décollement plunges southward into the subsurface.

After major offset along the décollement, rocks in the Snake Range were cut by steeply dipping normal faults in Miocene time and later that exhumed the range block (Miller et al., 1999; Rowley et al., 2017). Final uplift and exposure of the northern Snake Range occurred primarily during a regional episode of rapid extension in Miocene time (~17 Ma, Miller et al., 1999; Stockli, 2005; Colgan and Henry, 2009), prior to the formation of much of the present Basin and Range physiography of east-central Nevada.

Great Basin National Park consists of approximately 31,200 hectares (~312 km^2) of mountainous terrain in the southern Snake Range. In contrast to the mountain ranges of eastern Nevada and western Utah where Paleozoic carbonate rocks crop out, the southern Snake Range exposes some of the oldest rocks in the Basin and Range Province—Neoproterozoic and Lower Cambrian quartzite, argillite, and shale of the McCoy Creek Group overlain by the massive, generally cliff-forming Prospect Mountain Quartzite. These units are up to 2700-m thick and form most of the high peaks of the park. Overlying this siliciclastic succession is a thin interval of Cambrian Pioche Shale and middle Cambrian Pole Canyon Limestone, a 500-600-m thick, mostly massive limestone unit that has been metamorphosed to marble in the vicinity of Lehman Caves and is highly foliated. The Pole Canyon Limestone forms the hill in which the Lehman Caves has developed and underlies prominent hills to the southwest along Baker Creek and the lower reaches of Pole Canyon. The Pole Canyon Limestone, where highly fractured or where dissolution has enlarged the fractures and bedding planes, can transmit large quantities of water (Prudic et al., 2015).

Granitic rocks that range in age from Jurassic to Cenozoic intrude the Prospect Mountain Quartzite, Pioche Shale, and Pole Canyon Limestone in the southern Snake Range (Whitebread, 1969; McGrew et al., 1995). Most outcrops of granitic rocks in the Baker and Lehman Creek drainage basins near Lehman Caves belong to the late Eocene (36 Ma) Young Canyon pluton (Miller et al., 1999); the upper parts of this pluton invade the Pioche Shale as sill-like intrusive bodies west of Lehman Caves or form small, isolated exposures (McGrew et al., 1995).

Located in the northeast part of the park, Lehman Caves is small relative to other caves such as Mammoth Cave or Carlsbad Caverns, but it forms the largest cave system discovered in Nevada and it has an abundance of speleothems that make it one of the most decorated caves in the United States. The cave is between 15 to 70 m below land surface and has about three kilometers of irregularly shaped passages (Fig. 31). Lehman Caves occurs in a fault-bounded block of metamorphosed middle Cambrian Pole Canyon Limestone. Foliation here dips steeply, although the cave passages are nearly horizontal. This relation led geologists to propose that the cave passages formed late in the history of the range, after uplift and tilting of the bedrock (Lachniet and Crotty, 2017). About one kilometer to the south of Lehman Caves, several other caves are developed within the Pole Canyon Limestone along Baker Creek (Bridgemon, 1965). Elsewhere in the vicinity of the Snake Range, caves are developed in fault-bounded, tilted blocks of Paleozoic carbonate rocks that lie above the Snake Range Décollement, which bounds the east side of the range and dips gently eastward beneath Snake Valley. Cambrian and younger limestone and dolomite, more typical of other ranges in eastern Nevada and western Utah, are more extensive at the extreme south end of the park.

STOP 6. LEHMAN CAVES, NEVADA

Lehman Caves, located in east-central Nevada in the southern Snake Range (Fig. 4), was rediscovered in 1885 by Absalom Lehman, and much of the cave was explored that year. The cave had previously been known by local tribes. Major discoveries came later: The Lost River Passage in 1947 and the Gypsum Annex in 1952 (Great Basin National Park, 2019). Mr. Lehman quickly opened the cave beyond its first chamber and started guiding tours.

On January 24, 1922, President Warren G. Harding designated Lehman Caves National Monument to protect "certain natural caves, known as Lehman Caves…which are…of unusual scientific interest and importance…" Lehman Caves National Monument became incorporated into Great Basin National Park on October 27, 1986.

Lehman Caves is approximately three kilometers long, with one kilometer developed as a tourist trail (Fig. 31). It is relatively horizontal, although access was originally through a collapsed area about eight meters high, requiring ropes, ladders, or stairs to descend. Visited by about 33,000 visitors a year on ranger-guided tours, the cave is one of the main attractions at Great Basin National Park.

Stop 6.1. Entrance Tunnel

The Entrance Tunnel, constructed from 1936 to 1939, allows easy access to Lehman Caves. The cave is located at about 2070 m asl in the Pole Canyon Limestone, which is locally metamorphosed to a mylonitic marble.

Much of the cave is highly decorated with secondary speleothems. Of note are the abundant cave shields, welts, and turnip stalactites. The average cave temperature is 11°C, with relative humidity about 95%.

The areas along the cave tour route have seen disturbance over the years. The first cave trail was made of sand and sediment to flatten out areas, with asphalt added from 1955-58, and concrete on top of that in 1974. The first cave lighting system was installed in 1941 and replaced in 1977. Numerous areas of the cave were blasted over time to increase headroom and make the traverse easier (Great Basin National Park, 2019).

Lehman Caves is home to a variety of life. The Great Basin pseudoscorpion (*Microcreagris grandis* Muchmore) was discovered by Park Custodian T.O. Thatcher in 1930. It was later described as a species new to science and has only been found in a few caves in the southern Snake Range. Additional cave biota include bats, particularly Townsend's big-eared bats, the millipede *Idagona lehmanensis*, flies, beetles, springtails, and mites.

The cave is rich in paleontological resources in the form of faunal remains, with hundreds of bones found in 1937-38 and 1963 excavations. The predominant bones were jackrabbit, cottontail rabbit, and marmot (Rozaire, 1964).

Stop 6.2. Gothic Palace Through Tom Tom Room

Under the natural entrance in the winter months, one can often find mirabilite ($Na_2SO_4 \cdot 10H_2O$) on the wall. Continuing on to the Gothic Palace, the first major room of the tour route, the first impression is a church-like room full of a variety of speleothems. Looking more closely, one can see speleogen-forms of bedrock, some with bubble trails and boneyard. Along with more

common cave speleothems like stalactites and draperies, less familiar ones like helictites and shields extend from walls, ceilings, and floors.

Helictites are eccentric, linear, secondary growths that are usually composed of calcite and vary from hair-thin to several centimeters wide and up to a meter or more long. Common in Lehman, most grow out of other speleothems (e.g., columns, shields, and stalactites). Helictites form as capillary water oozing out of central channels evaporates or loses carbon dioxide. Curvature may be caused by impurities, crystallographic axis rotation, and stacking of wedge-shaped crystals (Hill and Forti, 1997).

A 1.5-m-diameter cave shield hangs from one wall of the Gothic Palace. Cave shields form as extensions of joints or cracks in the floor, wall, and ceiling in which calcite-rich water under hydrostatic pressure moves through the joints within the bedrock. Once the water exits the joint, it loses carbon dioxide to the cave chamber and precipitates calcite on either side of the joint… a planar example of the helictite-forming process. Lehman is internationally recognized for its abundance of shields, which Davis (2019) attributes to the extremely low, primary, permeability of the marble, and secondary permeability provided by an abundance of tectonic fractures. This large cave shield sports small calcite ridges representing internal paleo-waterlines (Fig. 32).

Continuing from the Gothic Palace, the next room is the Rose Trellis Room, full of helictites, broken speleothems with small, newer soda straws growing on them, and packrat middens. From here, the cave passage narrows, with up and down stairs until we reach the Tom Tom Room where there are numerous cave shields. It is easy to see the medial crack of several of them.

Stop 6.3. Base of Stairs into Lodge Room

Near the base of the stairs that lead up into the Lodge Room, one can find eight vertical holes in the flowstone. They are about 5-7 cm in diameter and up to 42-cm deep (Fig. 33). Nearby are coralloidal stalagmites with hollow interiors, similar to those at Stop 4.6.

Stair construction exposed a thick bed of massive white rock covered by extensive travertine with abundant, embedded soda straws fragments. Pseudoscallops are on walls and the ceiling surfaces. The uppermost part of the passage shows boneyard-like speleogens and extensive "punk rock," a product of condensation corrosion (Hill, 1987) (Fig. 34).

Stop 6.4. Talus Room at Entrance to Gypsum Annex

The next stop, the Talus Room, is different from the commercial part of the cave. The bedrock floor is probably about the same level as the rest of the cave but is covered by a 35-m-high pile of talus ("breakdown" - in speleological parlance) (Fig. 35). Speleothems (secondary cave deposits) are scarce. A few are scattered at the north and south end of the room. The only water is in perennial pools at the base of the talus pile, under the east wall. Several faults of unknown displacement crisscross the ceiling and one forms the west wall.

The Prospect Mountain Quartzite overlies this area on the surface (Fig. 36). Only recently recognized, the quartzite was likely a block transported during the décollement shearing event. The quartzite retards infiltration of meteoric waters into the northern part of the cave, preserving many pre-Pleistocene features. The part of the cave that lies beneath surface outcrops of Pole Canyon marble, including the entire commercial trail section, received vast amounts of meteoric

infiltration during the Pleistocene that removed all of the highly soluble gypsum and likely other soluble and/or soft minerals formed in the early speleogenetic phase.

Lehman Caves must be younger than 17 Ma, the age of the Snake Range décollement. Prominent joints and faults controlled the passage development. We will show that the cave formed near and just above the water table. Thus, speleogenesis must have followed, or likely accompanied, the uplift of the southern Snake Range. The main pulse of this uplift was 10 Ma and 8 Ma (Evans et al., 2015; Rowley, 2017), the probable age of the cavern.

Area uplift caused the water table to fall, removing buoyant support of water and hydrostatic pressure on the ceilings and walls. The most active period of ceiling collapse likely accompanied the de-watering of the cave millions of years ago. Erosion removed much of the overburden and released lithostatic pressure. The resulting expansion of bedrock fractures probably facilitated ceiling and wall collapses

Several varieties of gypsum are abundant in the northern part of the cave. Crystal wedging undoubtedly contributed to loosening of fractured blocks from the ceiling and contributed to the accumulation of breakdown. The conversion of limestone ($CaCO_3$) to the much larger gypsum ($CaSO_4 \cdot 2H_2O$) molecule is accompanied by significant expansion and prying within the bedrock, commonly resulting in breakdown on the floor and blocky domes in the ceiling. This is a common process in Mammoth Cave, Kentucky, for example. Today the Lehman Caves is not prone to ceiling or wall collapses and over 120 years of safe tours demonstrate that it is as, or probably more, stable than most mountainous recreation sites. Most of the collapse occurred millions of years ago.

Stop 6.5. Gypsum Annex Passage Split

Near the Gypsum Annex major junction is an area with distinctly undercut passage walls. Vertical channels (rills) are present above the undercut wall and pseudoscallops pock the down-facing inclined surface immediately above the old pool water line. Slightly below the pseudoscallops there is an incised horizontal water line or solution notch. The passage wall below the water line has no pseudoscallops. This site is the best example of an ancient acid pool basin in Lehman Caves (Fig. 37).

Acid pool basins in Lechuguilla cave are described by Davis (2000, p. 148) and in Carlsbad Cavern by Palmer and Palmer (2012). (Also see Stops 1.3, 2.2, 4.4, and 4.5 above.) These sites are where H_2S moved upward to the water table and was released into the cave atmosphere. Gaseous H_2S absorbed into oxygenated microdroplets of water in the atmosphere and into films of oxygenated condensation water on wall and ceiling surfaces, oxidizing it to H_2SO_4. Where the acid was in contact with limestone or dolomite, gypsum paste formed. The paste became progressively more acidic as H_2S reacted with oxygenated water mixed with the microcrystalline gypsum. The paste was quite moist, had no mechanical strength and tended to ooze and flow down walls, dissolving vertical rills in the process. On ceilings and overhanging walls, blobs of moist, acidic gypsum paste fell in response to gravity and either accumulated on passage floors or fell into pools where the acid was neutralized by reacting with the carbonate basin. Where acidic water trickled and oozed down the wall, the acid-carbonate reaction occurred at the edge of the pool, creating an undercut wall. If the acid reaction was particularly intense and persistent, a horizontal notch was dissolved at the top of the pool (Fig. 37).

One feature that has not been identified in the Gypsum Annex is the feeder source for H_2S. Carlsbad and Lechuguilla acid pool basins commonly have an enlarged vertical fracture in the floor, but no such feature has yet been identified in Lehman Caves. The marble of the Pole Canyon Formation that hosts the cave is intensely fractured, suggesting that H_2S could have risen to the water table along multiple fractures rather than at one primary vent.

Stop 6.6. Constriction in Gypsum Annex

This stop is at a section of the Gypsum Annex passage where the passage is lower and narrower than in the adjoining sections. Prominent features are wall crusts, bare rock and encrusted roof pendants, stalactites, trays, and hollow, calcite-encrusted drip tubes (Fig. 38). Some of the bare-rock roof pendants are short, projecting downward 10 to 15 cm below ceiling level. Stalactites are enlarged downward due to encrustation by botryoidal calcite. At the bottoms of stalactites are trays, similiar to those seen at Stop 3.2 and 4.8. The planar, down-facing surfaces of many of these trays are tilted about 5° from horizontal but the planes do not all tilt in the same direction. The direction of tilt appears to be related to the length of the pendant. On the floor are numerous conical hollow tubes encrusted with botryoidal calcite and up to 20-cm tall. Passage walls and roof pendants are covered with calcite crust that grades from about 1 mm to several cm thick. The ceiling is about 60% covered by crust and 40% bare bedrock.

Stop 6.7. Gypsum Annex Passage

Walking through the Gypsum Annex reveals much of the evidence of the cave's hypogenic, probable sulfidic and carbonic acid origins. The walls are coated with calcite and gypsum crusts partially detached from the bedrock. The floor is covered with the debris of fallen crust. The

relationship between the calcite crusts and gypsum is not clearly understood but both could have originated during the earliest stages of speleogenesis. A rimmed floor vent attests to the passage's hypogenic origins. Later deposits of gypsum flowers and aragonite crystals dot the walls.

Condensation corrosion has dramatically altered the surfaces of calcite speleothems, ceilings, and bedrock. Preferential growth of cave popcorn reveals the air-current patterns since the original dripstone formed. The popcorn-encrustations grew where moving air caused evaporation. Drying caused calcium carbonate-saturated water to be wicked to the dry surface where it deposited popcorn and coralloid speleothems. This resulted in preferential popcorn growth on the entrance-facing sides of walls, pendants, and speleothems (Hill, 1987).

Stop 6.8. Northern End of Gypsum Annex

Gypsum identified from the white deposits lining the trail could reveal a very interesting origin. If precipitated during an initial stage of sulfuric acid speleogenesis, the surface of these crusts, attached to the ceilings and walls at the time, would have been teeming with microorganisms. In caves actively forming through this process, sulfur-oxidizing bacteria and other microbes are able to "eat" sulfide gas (H_2S) and produce sulfuric acid (H_2SO_4), which corrodes limestone and leads to the gypsum precipitation under highly acidic conditions (pH <2 and sometimes below 0; see Stops 1 and 2.) Ongoing microbiological studies in the Gypsum Annex will describe the microbial species living in the sediments today and examine any preserved evidence that could indicate past microbial activity associated with sulfidic processes. Preliminary microbial community analysis indicates that these white sediments currently host very low microbial biomass, with microorganisms that live off very small amounts of organic carbon and inorganic

nitrogen, a far cry from the robust microbial communities that may have once thrived in this system.

At two locations along this passage, very small sections of the white floor deposits are tinged with a fluorescent yellow color; barely noticeable to the eye except under close examination. Scanning Election Microscopy with Energy-Dispersive X-ray Spectroscopy (SEM-EDS), which resolves images at very high magnification and provides elemental analysis, indicates the characteristic platy structure and uranium-vanadium character of what is presumed to be the mineral metatyuyamunite ($Ca(UO_2)2V_2O_8 \bullet 3(H_2O)$) that has been observed in some other ancient hypogene caves (Polyak and Mosch, 1995; Onac et al., 2001) (see Stops 3.7 and 4.7).

As the passage continues to the north, it eventually tightens and pinches out, with some small perennial drip pools at the end. Towards this end of the passage, more corrosion residues mar speleothem surfaces. The loose, dark brown/black sediment coats the popcorn speleothems at the base of the walls and appears to have sloughed off from above. These sediments have higher microbial biomass compared to the white deposits, perhaps due to a higher organic content.

Small pods of dark brown, shaly, clastic rock crop out at several locations within the Gypsum Annex. It appears that Pioche Shale was squeezed into fractures in the Pole Canyon marble when both formations were buried at greater depth.

A deposit of white paste-like material lies beneath a thin (1 mm) crust next to the marked trail. The crust apparently had been accidentally broken, but this fortuitously reveals the white paste, which appears to be a type of moonmilk of unknown composition. Moonmilk can be composed of calcite, hydrated carbonate minerals, or gypsum. The paste-like material in Gypsum Annex effervesced in 10% HCl, indicating that it is carbonate. Moonmilk is biogenic, forming by the

direct precipitation of calcite or where microbial bodies provide nucleation points where calcite can crystallize (Spilde et al., 2008).

Stop 6.9. North End of Talus Room

Several desiccated stubby stalagmites in the northern Talus Room have peculiar indentations centered in their tops (Fig. 39). These are probably drill holes formed mechanically by dripping water. Lehman Caves has several sites where drill holes occur, including early stage coralloid-encrusted drip tubes and holes mechanically drilled by dripping water. Although all are most likely associated with dripping water, their mode of origin is not the same. In the case of the mechanically drilled holes, there are questions about the composition of the material containing the holes, as well as questions about the acidity of the drip water.

Stop 6.10. Royal Gorge

This narrow, very high passage resembles a stream canyon, but there are no fluvial deposits. Instead, there is strong evidence of hypogenic origin. Like the Gypsum Annex and Talus Room, Royal Gorge is under the quartzite cover. Numerous cupolas dot the ceiling, a feature commonly associated with thermal, artesian, hypogene, or mixed-water origins (Osborne, 2004). There are also ceiling channels and drains. A secondary crust covers most of the passage walls. Much of it is detached from the bedrock, which happens when the original, moist, and possibly high biomass content dries out, dies off, and the crust contracts. The Royal Gorge crusts resemble gypsum crusts (lithified gypsum paste) that are common in active sulfidic caves but they react to 10% HCl, thus are thought to be now composed of calcite.

Stop 6.11. Grand Palace

At the end of the Royal Gorge, our tour crosses the Sunken Garden pools and ascends into the Grand Palace, one of the most decorated rooms in the cave and the highlight of the tourist route. If we could go straight up about 60 meters, we would reach the hill surface, covered by permeable Pole Canyon marble, which allows rainwater and meltwater to percolate through the rock and reach the cave below.

The Grand Palace is home to the spectacular Parachute shield, along with over 30 other shields. Numerous welts are also present, usually presenting as flat plates in the middle of a column. The cave ceiling has an abundant collection of turnip stalactites. These stalactites are 20-30 cm long, but have a bulge resembling a turnip at their middle or lower end. Broken turnip stalactites in another part of the cave show layers that resemble an onion. To our knowledge, turnip stalactites are only found in caves with cave shields.

Although most of the ceiling is covered with speleothems that hang, there is a big opening in the Grand Palace ceiling. This dome, or cupola, extends more than 10 m, narrowing as it reaches higher.

Stop 6.12. Rocky Road

Bubble trails and cupolas are speleogenetic features that form when early-stage cave passages are submerged (Audra et al., 2009). Near the air-water interface, carbon dioxide or hydrogen sulfide comes out of solution and forms bubbles which rise toward the surface due to buoyancy. The bubbles rise vertically until they encounter the hanging wall of a fissure or the overhung wall of a passage. They will then follow the wall upward until they reach the highest possible

point where they are trapped. If there is no trapping point, the bubbles will continue to rise to the water-air interface and disperse into the atmosphere. Acid gas will dissolve carbonate rock along the path followed by the bubbles, leaving an incised trail in the bedrock.

Cupolas are enigmatic features that may or may not be related to sulfuric acid speleogenesis speleogenesis. They are bell-shaped cavities in the ceilings of caves that could be gas traps within bedrock voids in the phreatic zone. Their origin is a subject of considerable debate (Osborne, 2004).

Stop 6.13. Inscription Room

Aside from the inscriptions, another signature of human presence is left on the ceiling in this area. Splotches of pink and orange cover parts of the ceiling, which are thought to be due to the growth of pigmented microorganisms. All throughout the cave, microbial life proliferates in areas touched by humans. Although the oils from human hands and skin cells don't seem very nutritious, they represent substantial energy resources for microorganisms that would otherwise not be able to proliferate in the very nutrient limited natural conditions of the cave, such as in the less-impacted Gypsum Annex (Stops 6.5 - 6.8). Old soot and waxes from historic light sources may also have contributed energy for these microbes.

The floor of the Inscription Room is mostly covered by flowstone with fragments of broken stalactites cemented in place. The flowstone has partly engulfed steeply conical coralloid-encrusted drip tubes, similar to those seen at Stop 6.6 in the Gypsum Annex. We believe that all of Lehman Caves once looked similar to the Gypsum Annex, but late-stage (Pliocene and Pleistocene) calcite deposition in the southern part of the cave has covered most of the features that formed during or shortly after the sulfuric acid speleogenetic event.

Stop 6.14. Lodge Room

On our way into the Lodge Room, we can see another indicator of human impact upon the cave microbiota. Artificial lights installed along the tour route provide an oasis for photosynthetic microorganisms, known as "lampenflora." Although the energy provided by these lights is less than 1% of the light energy that surface environments receive (Havlena et al., 2021), it still represents a substantial energy input to the cave ecosystem and, as a consequence, is easily exploited by light-harvesting organisms transported into the cave. Substantial time and resources are spent combating lampenflora, which are unsightly and can degrade speleothem surfaces.

The rectilinear pattern of Lehman Caves passages indicates that earliest dissolution of Pole Creek marble occurred along generally east- and north-trending joints. Bubble trails and perhaps cupolas suggest that early passage enlargement occurred in the phreatic zone. Based on early-stage indicators of gypsum, such as rills, trays, hollow coralloid-encrusted drip tubes, acid basins and pseudoscallops, initial passage enlargement was followed by a sulfuric acid speleogenetic event. Sulfuric acid speleogenesis implies that a falling water table intersected previously formed passages. In modern sulfuric acid speleogenesis caves, dissolution accompanied by precipitation of gypsum occurs at and slightly above the water table. Lehman Caves does not have known massive deposits of speleogenetic gypsum but does contain abundant secondary sulfuric acid speleogenesis indicators. Once the water table fell below the known passages in Lehman Caves, sulfuric acid speleogenesis ceased. A major research problem is identifying the source of the H_2S that caused sulfuric acid speleogenesis.

In the south (tourist trail) part of the cave, late-stage speleothems are abundant, covering most bedrock features and older speleothems. Carbon dioxide-driven condensation corrosion, best

seen in the Lodge Room, has modified bedrock and speleothems near the ceiling, giving formations a skeletal appearance and exposing etched Pole Canyon marble (Fig. 40).

Stop 6.15. Lodge Room to Exit Tunnel

The tourist trail leading to the exit tunnel was constructed in 1970. It includes a carved trench through a 0.5 to 1.0 m thick massive flowstone deposit, where some interesting curiosities are revealed. Currently unstudied and undated, this flowstone could contain data on Pleistocene or earlier climates. Within the flowstone, there are several places where the layers resemble stromatolites. Tucked into the flowstone are small, roofed-over paleo-pools that display calcite crystals resembling pool fingers, a type of speleothem associated with microbes in other caves. Reports of stromatolites within cave flowstone are rare but known (Melim et al., 2001; Rossi et al., 2010; Bontognali et al., 2016). As we leave the cave, we may see ephemeral (winter-only) mirabilite on the wall.

STOP 7. SNAKE CREEK (INDIAN) BURIAL CAVE, NEVADA

Snake Creek Burial Cave, sometimes referred to as Indian Burial Cave or Burial Cave, is the lowest-elevation cave on this field trip, at approximately 1700 m (Fig. 4). It is on Bureau of Land Management administered land. The entrance is a natural trap sinkhole with a 10-m pit into a large entrance room.

The cave has been known for hundreds if not thousands of years and has high cultural significance for area tribes. In the 1980s, paleontologists found a variety of fish, amphibian, reptile, and mammal remains of Pleistocene age. Of note are bones of horses, camels, and even a wolverine skull (Mead and Mead, 1989).

While this small cave has in the past received attention for its cultural uses and paleontological values, its geologic origins have not been well-explored. Because of its cultural artifacts and significance, entry is rarely permitted.

Geologic Setting

Burial Cave formed in the Middle to Late Devonian Guilmette Formation (McGrew et al., 1995), an extremely fractured limestone riddled with an extensive web of narrow calcite-filled veins at the cave site. The entrance room formed at the intersection of at least three, near-vertical, dip-slip faults. Two strike approximately west-to-east and the other approximately north-south. Rowley et al. (2017) mapped north-northwest-trending normal faults on each side of the elongated, narrow hill hosting Burial Cave, suggesting that the hill is a small horst elevated by Basin and Range faulting during the Miocene (~20-10 Ma) extensional phase.

Location

Burial Cave is located in a rocky outcrop about five kilometers west of Garrison, Utah, just over the state line in Nevada (Fig. 4). The cave is accessed via a gated entrance above a vertical drop.

Stop 7.1. Entrance Room

Entrance room (Fig. 41a) walls have a patina of flowstone, in some places eroded away to reveal a substrate of soft, punky rock that may be remnants of old gypsum paste. The walls show morphology strongly reminiscent of eroded gypsum paste in active sulfide-rich caves. The ceiling here and throughout the cave has numerous cupolas and likely “bubble trails”. Bubble trails are smoothed-wall, half-tubes on cave ceilings and overhanging walls commonly

interpreted as subaqueous and resulting from corrosion by ascending carbon dioxide bubbles seeking the steepest available path and locally increasing the acidity of the water (Audra et al., 2009).

Stop 7.2. Downward-Trending Passage

The entrance room leads into a narrow downward-trending passage, which is dramatically different from the entrance room. The walls are mostly coated by mammillaries and folia. Mammillaries form below the water table in quiet water supersaturated with calcite. Folia also form in quiet, high-CO_2, calcite-supersaturated water but within a few meters below the water table. Folia grow over the mammillaries where both are present. Mammillaries are more commonly exposed higher in the passage with the folia (covering mammillaries) more concentrated in the lower part of the passage (Fig. 42). In active settings, folia typically grow in water with cave rafts on the surface (Palmer, 2007, p. 277). When associated with bubble trails, as seen in Burial Cave, Audra et al. (2009) view folia as indicators of hypogenic speleogenesis.

Corrosive water vapor condensing on the cave walls has dissolved folia and mammillaries in the lower cave, particularly on the west wall. Condensation corrosion is typical in active and inactive hypogenic caves in dry climates (Dublyansky and Dublyansky, 2000).

STOP 8. CRYSTAL BALL CAVE, UTAH

Crystal Ball Cave is a small, beautiful, hypogenic cave hosting a wide variety of unique features that illuminate the region's past. A local ranch family provides tours through the cave and have for many years. They provide visitors with a basic understanding of the cave's development and point out its unique features. The cave is approximately 150 m long (Fig. 41b) and known for its

spectacular nail head (rhombohedral), calcite spar that coats the cave walls, floor, and ceiling like a large geode (Fig. 43). The cave also preserved a wide variety of Pleistocene fossils including saber-toothed cat, camel, "large-headed llama," and musk ox. The rich faunal and floral assemblage can be attributed to the cave's proximity to the former Lake Bonneville that was within two kilometers of the cave when it was at its highest level about 25,000 years ago (Heaton, 1985).

Geologic Setting

The cave developed along a high-angle normal fault within the middle Cambrian Notch Peak Limestone Formation and is situated in the upper plate of the northern Snake Range décollement (Gans et al., 1999a). The cave's origin was likely concurrent with Basin and Range tectonics and involved deep-seated acid sources (CO_2-H_2S) when the cave was located below the water table (Decker et al., 2015). As the Basin and Range landscape formed, the water table dropped below the level of the cave, ending primary speleogenesis.

Location and Route to Cave

Crystal Ball Cave is located on Spring (aka Gandy) Mountain just across the Nevada border in Utah (Fig. 4). Visitors follow a guide on a rudimentary trail through the cave to the blasted exit and bring their own lights. Reservations are required. More information can be found on the Crystal Ball Cave website, by calling 801-787-6675, or using Facebook Messenger.

Stop 8.1. East Entrance Room

The most noticeable geologic features in the cave are calcite coatings precipitated on the cave walls, particularly nail-head spar and mammillaries, that likely precipitated in shallow, saturated conditions as the water table dropped. Their abundance gives the feel of walking in a giant geode. The crystal "balls" are large breakdown blocks coated with the spar (Fig. 43). Gilleland and Rogers (2016) reported that the cores of many "balls" are partly made of anauxite, a clay mineral commonly associated with thermal water alteration. Other abundant hypogenic cave features including cupolas, vents, and bubble trails are also coated with spar, indicating that the spar precipitated during or after a late stage of hypogene cave development.

Although the presence of gypsum on the floor suggests that sulfuric acid speleogenesis may have occurred near a paleo-water table, as proposed for other caves in the region, the gypsum overlies relatively uncorroded-looking spar. Thus, the gypsum may have formed by late-stage ponding of gypsum supersaturated waters. Once the cave was exposed to the surface, there were opportunities for a variety of flora and fauna to enter the cave or be carried in and preserved in perpetuity.

Bruce Rogers (personal communication, 2020) suggests that the cave initially formed from mixing of descending epigenic water with ascending thermal water, forming the passages with cupolas, bubble trails, and vents. As the water table lowered, much of the breakdown fell. Later, the thermal water table rose again as a supersaturated solution and deposited the nail-head spar calcite throughout the cave. After the cave drained, calcite dripstone, aragonite crystals, and gypsum crusts, needles, and floor deposits developed in the subaerial environment.

STOP 9. PESCIO CAVE, NEVADA

Geologic Setting and Location

Pescio Cave formed in a Cambrian, Pole Canyon-equivalent limestone (Hose and Blake, 1970) on the lower, western flank of the Schell Creek Range only about a dozen miles from Monte Neva Hot Springs (Fig. 4). The current Steptoe Valley has demonstrated subterranean, CO_2-rich, hydrothermal resources (Nevada Bureau of Mines and Geology, 2010). The western border of the Schell Creek Range is bound by a Cenozoic normal fault that dropped the Steptoe Valley relative to the mountain range. The cave is about 240 m long (Fig. 41c).

Stop 9.1. Entrance Room

The entrance room is well-lit in daytime by the ~2.5- x 4-m entrance. Its most notable feature is a large stalagmite in the middle of the room abundantly coated with amberat (desiccated wood rat urine). The entire floor is covered with packrat midden as are ceiling-tube floors.

The passage narrows and bifurcates about 25 meters into the cave. Both passages show evidence of hypogenic origin and aggressive aerial condensation corrosion. Heavily weathered mammillaries, typically associated with hypogenic origins, line the walls. These are likely the oldest speleothems in the cave. Where the two passages come together at the east end, a ceiling channel, an apparent bubble trail, and a cupola are evident.

Stop 9.2. Coral Forest

The room of greatest interest is the Coral Forest, a large room making up the southeastern part of the cave. To the eye of someone familiar with sulfuric acid speleogenesis caves in the Guadalupe Mountains, Cueva de Villa Luz, and Frasassi Cave, the morphology of the uneven floor strongly

resembles rooms with massive speleogenetic gypsum, suggesting that this floor was once covered by massive gypsum sediments that sloughed-off the ceiling and walls during the earliest sub-aerial development of the cave. A small area of apparent remnant gypsum (no reaction to 10% HCl, softer than a fingernail) supports this hypothesis.

As demonstrated in the Guadalupe Mountain caves (Stops 3.3-3.4 and 4.6), speleogenetic gypsum masses ("glaciers") can be locally dissolved by dripping water that quickly bores a hole, creating a drip tube. The gypsum immediately adjacent to the drip hole becomes denser by recrystallization, effectively case-hardening the tube. If the drip tube linings remain coupled to the cave floor after gypsum has been removed, calcium-carbonate-saturated water can be wicked upward through the tube wall where it precipitates as aragonite and botryoidal calcite. The resultant coralloid speleothem is, in essence, a fossilized drip hole.

We interpret the origin of the Coral Forest to have followed this process of speleogenetic gypsum, partially dissolved and partially replaced by calcite. Coralloid stalagmites are plentiful and, even more compelling are the numerous encrusted drip tubes (Fig. 44). The Coral Forest room is a spectacular display of these features, and it is possible that all of the coralloidal stalagmites without obvious central tubes also formed by this method.

STOP 10. DISCOVERY CAVE, NEVADA

Discovery Cave is a small, well-decorated, hypogene cave that is approximately 200-m long (Fig. 41d) and displays unique speleothems such as directional coralloid growth on stalactites and stalagmites, spherical quill anthodites, hydromagnesite balloons, folia, and mammillaries. Although no compelling evidence of sulfuric acid speleogenesis development has been identified

in the cave, a hypogene source with carbonic, and possibly sulfuric, acid formed this cave prior to ~8 Ma.

General Locality

Discovery Cave is located in the rugged landscape of the northern Snake Range in the Humboldt-Toiyabe National Forest in east-central Nevada (Fig. 4). The entrance is gated to protect the cave's fragile nature and unique speleothems.

Geologic Setting

Discovery Cave formed in middle Cambrian limestones (Gans et al., 1999b) and likely developed when the water table was at or just above the current cave level, concurrent with Basin and Range tectonics, which are reported to have been ~10-8 Ma in this area (Evans et al., 2015; Rowley, 2017). As the Snake Range rose, the water table dropped through the cave's level, depositing mammillaries, folia, and other unique speleothems.

Stop 10.1. Entrance Room

Mammillaries at the entrance and elsewhere in Discovery Cave, provide evidence of hypogenic origins. The mammillaries formed just below the water table and then were heavily corroded by carbonic and/or sulfuric acid condensate once they were exposed above the water table.

Stop 10.2. Main Room

Calcite folia on the southeast wall of the room and in the adjacent alcove overlie the calcite mammillaries, similar to their relationship at Burial Cave, but the folia here consistently dip 6^{o} in the direction 270^{o} (Fig. 45). Actively growing calcite folia form within the upper 10 meters of a fluctuating water table, or less often very slow-moving pool of water. The calcite folia in

Discovery Cave formed near the top of the retreating water table as the cave drained. Thus, the folia formed during uplift and tilting of the northern Snake Range.

Numerous ceiling cupolas and the overall ramiform pattern of the cave suggest sulfuric acid speleogenesis (Palmer, 2007).

STOP 11. OLD MANS CAVE

Old Mans Cave is a small hypogene cave developed along high-angle normal faults situated in the upper plate of the northern Snake Range décollement. The cave is approximately 860 m long and displays classic features related to hypogene (Fig. 41e), although not necessarily sulfuric acid, speleogenesis.

General Locality

Old Man Cave is in east-central Nevada, within the Humboldt-Toiyabe National Forest on the south end of the northern Snake Range (Fig. 4). The entrance has been gated to restrict visitation during the summer bat maternity roosting period. Access and permit information is available at the United States Forest Service, Ely Ranger District in Ely, Nevada.

Geologic Setting

Old Mans Cave developed in the Cambrian Notch Peak Limestone Formation (Miller and Gans, 1999) along vertical normal faults that exhibits brecciated zones throughout much of the cave. The cave's origins likely began concurrent with Basin and Range tectonics (about 10-8 Ma) when the area was below the water table. The cave developed under complex hypogene processes involving deep-seated acidic sources, likely originating from tectonic/igneous activity that drove corrosive fluids from below (Audra, 2017). As the basin floor dropped and the Snake

Range rose, the top of carbon dioxide-rich, and possibly sulfidic, waters dissolved the cave during the primary phase of speleogenesis.

Stop 11.1. **Boneyard Room**

Old Mans Cave is an outstanding example of hypogene speleogenesis that exhibits some exceptional boneyard features (also known as spongework). Well-developed keyhole passages, condensation corrosion, rills, cupolas, and ceiling domes and channels are featured throughout the cave (Fig. 46a and b). Floor vents along vertical faults provided pathways for corrosive fluids to well up during speleogenesis and deposit iron-oxide by-products within fault breccias. The cave walls are corroded and punky in texture except in areas where mammillary calcite has survived condensation corrosion and areas where secondary speleothems have developed post-speleogenesis.

Stop 11.2. **Breakdown Room**

White calcite deposits here and elsewhere in the cave resemble gypsum pastes and crusts in other caves in the region, although recent XRD and SEM analysis by Havlena and Jones (unpublished results) have shown the material to be calcite. To date, the only gypsum identified in the cave consists of small needles in clastic sediments near the dry pool south of this stop. They are interpreted to represent recent secondary precipitates.

Stop 11.3. Lower Level

The type location for cave coral pipes (Fig.47a) is displayed on the slope of a stalagmite. Based on thin-section examination of a sample here as well as observations of actively growing coral pipes in a Grand Canyon cave, Hose and Strong (1983) concluded that the coral pipes formed in a manner similar to hoodoos. Easily eroded sediment protected by a more resistant capstone

eroded to form hoodoo-like pillars a few centimeters tall. Ultimately, however, the splash of the drips precipitated thin coats of calcite, thus lithifying the pillars. Initially, the sediments were interpreted as silt, but the geomorphology of the slope below the coral pipes suggests that the soft material may have instead been gypsum paste or moonmilk (Fig. 47b). Coral pipes, although uncommon, have been identified with initial cores of silt, monohydrocalcite moonmilk, gypsum, and bat guano (Hill and Forti, 1997).

ACKNOWLEDGMENTS

The authors thank our three reviewers, Paul Burger, Donald G. Davis, and Art Palmer, for their thorough comments. We also thank the photographers and cartographers who contributed to the figures used in this paper. Their names are listed in the captions. Many cavers also contributed to the maps and photographs by surveying, standing as models, and holding flashes. Regrettably, we do not have a complete list of these folks but, nonetheless, appreciate their help.

Our work in the various caves was possible through the support of Great Basin National Park, U.S. Forest Service – Ely Ranger District, Bureau of Land Management – Bristlecone Field Office, and Carlsbad Caverns National Park. DSJ and ZH thank New Mexico Tech, the National Cave and Karst Research Institute (NCKRI), and NASA Exobiology Program (80NSSC20K0619) for support, and ZH thanks the Rocky Mountain Association of Geologists for supporting her with the Gary L. Babcock Memorial Scholarship.

REFERENCES CITED

Armstrong, R.L., and Ward, P., 1991, Evolving geographic patterns of Cenozoic magmatism in the North American Cordillera: The temporal and spatial association of magmatism and

metamorphic core complexes: Journal of Geophysical Research, v. 96, p. 13201–13224, doi:10.1029/91JB00412.

Audra, P., 2017, Hypogene caves in France, *in* Klimchouk, A., Palmer, A.N., De Waele, J., Auler, A.S., and Audra, P., Hypogene Karst Regions and Caves of the World: Cham, Switzerland, p.61-83.

Audra, P., Mocochain, L., Bigot J.-Y., and Nobécourt J.-C., 2009, The association between bubble trails and folia: A morphological and sedimentary indicator of hypogenic speleogenesis by degassing, example from Adaouste Cave (Provence, France): International Journal of Speleology, v. 38, P. 93-102.

Barton, H.A., Bristol, D., and Hunter, J., 2020, Higher Education, Lechuguilla Cave: NSS News, v. 78, no. 11, p. 23-27.

Belcher, W.R., Elliot, P.E., and Geldon, A.L., 2001, Hydraulic-property estimates for use with a transient ground-water flow model of the Death Valley regional ground-water flow system, Nevada and California: U.S. Geological Survey Water-Resources Investigations Report 01–4210, 28 p, https://doi.org/10.3133/wri014210.

Best, M.G., and Christiansen, E.H., 1991, Limited extension during peak Tertiary volcanism, Great Basin of Nevada and Utah: Journal of Geophysical Research, v. 96, p. 13509, doi:10.1029/91JB00244.

Bontognali, T.R.R., D'Angeli, I.M., Tisato, N, Vasconcelos, C., Bernasconi, S.M., Gonzales, E.R.G., and De Waele, J., 2016, Mushroom speleothems: Stromatolites that formed in the absence of phototrophs: Frontiers in Earth Sciences, v. 4, no. 49, 8p. doi: 10.3389/feart.2016.00049

Bridgemon, R.R., 1965, The caves of Baker Creek with reference to the Baker Creek cave system, White Pine County, Nevada: Tucson, Arizona, University of Arizona Association of Cavers Grotto of the National Speleological Society, Arizona Caver, v. 2, no. 4, p. 45–79.

Brooks, W.E., Thorman, C.H., and Snee, L.W., 1995, Ar ages and tectonic setting of the middle Eocene northeast Nevada volcanic field: Journal of Geophysical Research, v. 100, p. 10403–10416, doi:10.1029/94JB03389.

Cohen, K.M., Finney, S.C., Gibbard, P.L., and Fan, J.X., 2013, The ICS International Chronostratigraphic Chart: Episodes, v. 36, p. 199-204, https://stratigraphy.org/ICSchart/Cohen2013_Episodes.pdf (accessed January 2021).

Colgan, J.P., and Henry, C.D., 2009, Rapid middle Miocene collapse of the Mesozoic orogenic plateau in north-central Nevada: International Geology Review, v. 51, p. 920–961, doi:10.1080/00206810903056731.

Cook, H.E., and Corboy, J.J., 2004, Great Basin Paleozoic carbonate platform: facies, facies transitions, depositional models, platform architecture, sequence stratigraphy and predictive mineral host models—Field trip guidebook: Metallogeny of the Great Basin Project, August 17-22, 2003: U.S. Geological Survey Open-File Report 2004-1078, 129 p, https://doi.org/10.3133/ofr20041078.

Curl, R.L., 1974, Deducing flow velocity in cave conduits from scallops: National Speleological Society Bulletin, v. 26, no., 2, p. 1-5.

Cyr, A. J., and Granger, D. E., 2008, Dynamic equilibrium among erosion, river incision, and coastal uplift in the northern and central Apennines, Italy: Geology, v. 36, no. 2, p. 103-106.

D'Angeli, I.M., DeWaele, J., Melendres, O.C., Tisato, N., Gonzales, E.R.G., Bernasconi, S. M., Torriani, S., and Bontognali, T.R.R., 2015, Genesis of folia in a non-thermal epigenic cave (Matanzas, Cuba): Geomorphology, v. 228, p. 525-535, http://dx.doi.org/10.1016/j.geomorph.2014.09.006.

D'Auria, G., Artacho, A., Rojas, R. A., Bautista, J. S., Méndez, R., Gamboa, M. T., Gamboa, J. R., and Gómez-Cruz, R., 2018, Metagenomics of bacterial diversity in Villa Luz caves with sulfur water springs: Genes, v. 9, no. 1, p. 55.

Dattagupta, S., Schaperdoth, I., Montanari, A., Mariani, S., Kita, N., Valley, J. W., and Macalady, J. L., 2009, A novel symbiosis between chemoautotrophic bacteria and a freshwater cave amphipod: The ISME Journal, v. 3, no. 8, p. 935-943.

Davis, D.G., 1973, Sulfur in Cottonwood Cave, Eddy County, New Mexico: National Speleological Society Bulletin, v. 35, p. 89-95.

Davis, D.G., 1980, Cave development in the Guadalupe Mountains: A critical review of recent hypotheses: NSS Bulletin, v. 42, p. 42-48.

Davis, D.G., 2000, Extraordinary features of Lechuguilla Cave, Guadalupe Mountains, New Mexico: Journal of Cave and Karst Studies, v. 62, p. 147-157.

Davis, D.G., 2012, In defense of a fluctuating-interface, particle-accretion origin of folia: International Journal of Speleology, v. 41, 189-198, http://dx.doi.org/10.5038/1827-806X.41.2.6 (accessed November 2020).

Davis, D.G., 2019, Helictites and related speleothems: Cave Shields, *in* White, W.B., Culver, D.C., and Pipan, T., Encyclopedia of Caves: Academic Press, London, p. 515-517.

Decker, D.D., Polyak, V.J., and Asmerom, Y., 2015, Depth and timing of calcite spar and "spar cave" genesis: Implications for landscape evolution studies, *in* Feinberg, J., Gao, Y., and Alexander, E.C., Jr., eds., Caves and Karst Across Time: Geological Society of America Special Paper 516, p. 103–112, doi:10.1130/2015.2516(08).

Dettinger, M.D., Harrill, J.R., Schmidt, D.L., and Hess, J.W., 1995, Distribution of carbonate-rock aquifers and the potential for their development, southern Nevada and adjacent parts of California, Arizona, and Utah; 1995: U.S. Geological Survey Water Resources Investigations Report 91–4146, 100 p., https://doi.org/10.3133/wri91414

Doucette, D., 1993, Chocolate High, Carlsbad Cavern – A preliminary report: NSS News, v. 51, p. 184-185.

Dublyansky, V.N., and Dublyansky, Y.V, 2000, The role of condensation in karst hydrogeology and speleogenesis, *in* Klimchouk, A., Ford, D., Palmer, A, and Dreybrodt (eds.), Speleogenesis: Evolution of Karst Aquifers: Huntsville, Alabama, National Speleological Society, p. 100-112.

DuChene, H.R., and Cunningham, K. I., 2006, Tectonic influences on speleogenesis in the Guadalupe Mountains, New Mexico and Texas, *in* Land, L., Lueth, V.W., Raatz, W., Boston, P., and Love, D.L. (eds.), Caves and Karst of Southeast-central New Mexico: New Mexico Geological Society 57th Annual Fall Field Conference Guidebook, p. 211-217.

DuChene, H.R., and Martinez, Ruben, 2000, Post-speleogenetic erosion and its effect on cave development in the Guadalupe Mountains, New Mexico and west Texas: Journal of Cave and Karst Studies, v. 62, p.75-79.

DuChene, H.R., Palmer, A.N., Palmer, M.V., Queen, J.M., Polyak, V.J., Decker, D.D., Hill, C.A., Spilde, M., Burger, P.A., Kirkland, D.W., and Boston, P., 2017, Hypogene speleogenesis in the Guadalupe Mountains, New Mexico and Texas, USA, *in* Klimchouk, A., Palmer, A.N., De Waele, J., Auler, A.S., and Audra, P., Hypogene Karst Regions and Caves of the World: Cham, Switzerland, p. 511-530.

Eaton, G.P., 2008, Epeirogeny in the Southern Rocky Mountains region: Evidence and origin: Geosphere, v. 4, p. 764–784, doi: https://doi.org/10.1130/GES00149.1 (accessed January 2021).

Egemeier, S.J., 1971, A comparison of two types of solution caves: Unpublished report to Carlsbad Caverns National Park, April 12, 1971, 7 p.

Egemeier, S.J., 1987, A theory for the origin of Carlsbad Caverns: National Speleological Society Bulletin, v. 49, p. 73-76.

Evans, S. L., Styron, R. H., van Soest, M. C., Hodges, K. V., and Hanson, A. D., 2015, Zircon and apatite (UTh)/He evidence for Paleogene and Neogene extension in the Southern Snake Range, Nevada, USA: Tectonics, v. 34, p. 2142-2164, file:///C:/Users/hose/Downloads/2015TC003913.pdf (accessed November 2020).

Galdenzi, S., Cocchioni, M., Morichetti, L., Amici, V., and Scuri, S., 2008, Sulfidic ground-water chemistry in the Frasassi caves, Italy: Journal of Cave and Karst Studies, v. 70, no. 2, p. 94-107.

Galdenzi, S. and Jones, D.S., 2017, The Frasassi Caves: A “classical” active hypogenic cave, *in* Klimchouk, A., Palmer, A.N., De Waele, J., Auler, A.S., and Audra, P., Hypogene Karst Regions and Caves of the World: Cham, Switzerland, p. 143-159.

Galdenzi, S., and Maruoka, T., 2003, Gypsum deposits in the Frasassi Caves, central Italy: Journal of Cave and Karst Studies, v. 65, no. 2, p. 111-125.

Galdenzi, S., and Sarbu, S., 2000, Chemiosintesi e speleogenesi in un ecosistema ipogeo: i rami sulfurei delle Grotte di Frasassi (Italia Centrale): Le Grotte d'Italia, v. 1, p. 3-18.

Gans, P.B., Miller, E.L., McCarthy, J., and Ouldcott, M.L., 1985, Tertiary extensional faulting and evolving ductile-brittle transition zones in the northern Snake Range and vicinity: New insights from seismic data: Geology, v. 13, p. 189, doi:10.1130/0091-7613(1985)13<189:TEFAED>2.0.CO;2.

Gans, P.B., Mahood, G.A., and Schermer, E., 1989, Synextensional magmatism in the Basin and Range province—A case study from the east-central Great Basin: Geological Society of America Special Paper 233, 53 p.

Gans, P.B., Miller, E.L., and Lee, J., 1999a, Geologic Map of the Spring Mountain Quadrangle, Nevada and Utah: Nevada Bureau of Mines and Geology, Field Studies Map 18, scale 1:24000, 12 p.

Gans, P.B., Miller, E.L., Huggins, C.C, and Lee, J., 1999b, Geologic Map of the Little Horse Canyon Quadrangle, Nevada and Utah, Nevada Bureau of Mines and Geology, Field Studies Map 20.

Garofano, M., and Govoni, D., 2012, Underground geotourism: A historic and economic overview of show caves and show mines in Italy: Geoheritage, v. 4, no. 1-2, p. 79-92.

Gilleland, T., 2016, and Rogers, B., Crystal Ball Cave (Utah), *in* Hoke, R., ed., 2016 NSS Convention Guidebook: National Speleological Society, p. 130-133.

Great Basin National Park, 2019, Lehman Caves Management Plan: Baker, Nevada, Great Basin National Park, 150p, http://npshistory.com/publications/grba/cave-mgt-plan-ea-draft-2019.pdf (accessed November 2020).

Grier, S.P., 1984, Alluvial fan and lacustrine carbonate deposits in the Snake Range: A study of Tertiary sedimentation and associated tectonism: Stanford, Calif., Stanford University, unpubl. M.S. thesis, 61 p.

Harrill, J.R., Gates, J.S., and Thomas, J.M., 1988, Major ground-water flow systems in the Great Basin region of Nevada, Utah, and adjacent states: U.S. Geological Survey Hydrologic Investigations Atlas HA-694-C, scale 1:1,000,000, 2 sheets, https://doi.org/10.3133/ha694C.

Harrill, J.R., and Prudic, D.E., 1998, Aquifer systems in the Great Basin region of Nevada, Utah, and adjacent States—Summary report: U.S. Geological Survey Professional Paper 1409-A, 66 p., https://doi.org/10.3133/pp1409A.

Havlena, Z.E., Kieft, T., Veni, G., Horrocks, R., and Jones, D.S., 2021, Lighting effects on the development and diversity of photosynthetic biofilm communities in Carlsbad Cavern, New Mexico: Applied and Environmental Microbiology, DOI: 10.1128/AEM.02695-20, https://pubmed.ncbi.nlm.nih.gov/33452019/ (accessed January 2021).

Hayes, P.T., 1964, Geology of the Guadalupe Mountains, New Mexico: U.S. Geological Survey, Professional Paper 446, 69 p.

Heaton, T.H., 1985, Quaternary Paleontology and Paleoecology of Crystal Ball Cave, Millard County, Utah: With emphasis on mammals and description of a new species of fossil skunk: The Great Basin Naturalist, v. 45, p. 337-390.

Heilweil, V.M., and Brooks, L.E., eds., 2011, Conceptual model of the Great Basin carbonate and alluvial aquifer system: U.S. Geological Survey Scientific Investigations Report 2010-5193, 191 p., https://doi.org/10.3133/sir20105193.

Hill, C.A., 1987, Geology of Carlsbad Cavern and other caves in the Guadalupe Mountains, New Mexico and Texas: New Mexico Bureau of Mines and Mineral Resources Bulletin 117, 150 p.

Hill, C.A., and Forti, P., 1997, Cave Minerals of the World, 2nd edition: National Speleological Society, Huntsville, AL.

Hintze, L.F., and Davis, F.D., 2003, Geology of Millard County, Utah: Utah Geological Survey Bulletin 133, 305 p.

Hose L.D., and Rosales-Lagarde, L., 2017, Sulfur-rich caves of southern Tabasco, Mexico, *in* Klimchouk, A., Palmer, A.N., De Waele, J., Auler, A.S., Audra, P. (eds) Hypogene Karst Regions and Caves of the World. Cave and Karst Systems of the World. Springer, Cham, Switzerland, p. 803-814. https://link.springer.com/chapter/10.1007/978-3-319-53348-3_54 (accessed January 2021).

Hose, L. D., Palmer, A. N., Palmer, M. V., Northup, D. E., Boston, P. J., and DuChene, H.R., 2000, Microbiology and geochemistry in a hydrogen sulfide-rich, karst environment: Chemical Geology: Special Geomicrobiology Issue, v. 169, p. 399-423, http://www.sciencedirect.com/science/article/pii/S0009254100002175?via%3Dihub (accessed November 2020).

Hose, L.D., and Pisarowicz, J.A., 1999, Cueva de Villa Luz, Tabasco, Mexico: Reconnaissance study of an active sulfur spring cave and ecosystem: Journal of Cave and Karst Studies, v. 61, p. 13-21.

Hose, L. D., and Strong, T. R., 1983, How coral pipes form: The NSS Bulletin, v. 45, p. 12-13.

Hose, R. K., and Blake, M.C., Jr., 1970, Geologic map of White Pine County, Nevada (East Half): Open-File Report 70-166, U.S. Geological Survey.

Jagnow, D.H., 1977, Geologic factors influencing speleogenesis in the Capitan Reef complex, New Mexico and Texas [M.S. Thesis]: Albuquerque, University of New Mexico, 197 p.Jones, D. S., and Macalady, J. L., 2016, The snotty and the stringy: Energy for subsurface life in caves, *in* Hurst, C. J., ed., Their World: A Diversity of Microbial Environments, Springer, p. 203-224.

Kellogg, H.E., 1963, Paleozoic stratigraphy of the southern Egan Range, Nevada: Geological Society of America Bulletin, v. 74, no. 6, p. 685-708.

Jones, D. S., Polerecky, L., Galdenzi, S., Dempsey, B. A., and Macalady, J. L., 2015, Fate of sulfide in the Frasassi cave system and implications for sulfuric acid speleogenesis: Chemical Geology, v. 410, p. 21-27.

Klatt, J. M., Meyer, S., Häusler, S., Macalady, J. L., De Beer, D., and Polerecky, L., 2016, Structure and function of natural sulphide-oxidizing microbial mats under dynamic input of light and chemical energy: The ISME Journal, v. 10, no. 4, p. 921-933.

Lachniet, M.S., and Crotty, C.M., 2017. Lehman Caves are likely older than 2.2 million years: Report to Great Basin National Park from Department of Geoscience, University of Nevada-Las Vegas, https://lachnietblog.wordpress.com/2017/02/01/lehman-caves-nevada-are-older-than-2-2-million-years/.

Lee, D.E., and Van Loenen, R.E., 1971, Hybrid granitoid rocks of the Southern Snake Range, Nevada: U.S. Geological Survey Professional Paper 668, 48 p.

Lee, D.E., Kistler, R.W., Friedman, Irving, and Van Loenen, R.E., 1981, Two-mica granites of northeast-central Nevada: Journal of Geophysical Research, v. 86, no. B11, p. 10,607–10,616, doi:10.1029/JB086iB11p10607.

Lee, J., and Sutter, J.F., 1991, Incremental 40 Ar/ 39 Ar thermochronology of mylonitic rocks from the Northern Snake Range, Nevada: Tectonics, v. 10, p. 77–100, doi:10.1029/90TC01931.

Macalady, J.L., Dattagupta, S., Schaperdoth, I., Jones, D.S., Druschel, G.K., and Eastman, D., 2008, Niche differentiation among sulfur-oxidizing bacterial populations in cave waters: The ISME Journal, v. 2, no. 6, p. 590-601.

Macalady, J.L., Mainiero, M., and Galassi, D.M.P., 2019, Chapter 52 - The Frasassi Caves, Italy, *in* White, W.B., Culver, D.C., and Pipan, T., eds., Encyclopedia of Caves (Third Edition), Academic Press, p. 435-443.

Mariani, S., Mainiero, M., Barchi, M., Van Der Borg, K., Vonhof, H., and Montanari, A., 2007, Use of speleologic data to evaluate Holocene uplifting and tilting: An example from the Frasassi anticline (northeast-central Apennines, Italy): Earth and Planetary Science Letters, v. 257, no. 1-2, p. 313-328.

Martini, J., 1986a, Report on the cave intersected by the Mostert adit in the Thabazimbi iron mine, and its possible management: South African Spelaeological Association Bulletin, v. 27, p. 1-6.

Martini, J., 1986b, The tray: An example of evaporation-controlled speleothems: South African Spelaeological Association Bulletin, v. 27, p. 46-51.

McGrew, A.J., Miller, E.L., and Brown, J.L., compilers, 1995, Geologic map of Kious Spring and Garrison 7.5' quadrangles, White Pine County, Nevada and Millard County, Utah: U.S. Geological Survey Open-File Report 95–10, scale 1:24,000, https://doi.org/10.3133/ofr9510.

Mead, E.M., and Mead, J.I., 1989. Snake Creek Burial Cave and a review of the Quaternary mustelids of the Great Basin: Great Basin Naturalist, v. 49, n. 2, p. 143–154, https://ojs.lib.byu.edu/spc/index.php/wnan/article/view/28786 (accessed November 2020).

Melim, L.A., Shinglman, K.M., Boston, P.J., Northup, D.E., Spilde, M.N., and Queen, J.M., 2001, Evidence for microbial involvement in pool finger precipitation, Hidden Cave, New Mexico: Geomicrobiology Journal, v. 18, p. 311–329, doi: 10.1080/01490450152467813.

Mifflin, M.D., 1968, Delineation of ground-water flow systems in Nevada: University of Nevada Desert Research Institute Technical Report H-W no. 4, 112 p.

Miller, E.L., Dumitru, T.A., Brown, R.W., and Gans, P.B., 1999, Rapid Miocene slip on the Snake Range-Deep Creek Range fault system, east-central Nevada: Geological Society of America Bulletin, v. 111, p. 886-905.

Miller, E.L., and Gans P.B., 1999, Geologic map of The Cove quadrangle, Nevada and Utah: Nevada Bureau of Mines and Geology, Field Studies Map 22z.

Miller, E.L., Gans, P.B., and Garing, J., 1983, The Snake Range Décollement: An exhumed Mid-Tertiary ductile-brittle transition: Tectonics, v. 2, p. 239, doi:10.1029/TC002i003p00239.

Montanari, A., Lüthgens, C., Lomax, J., Mainiero, M., Mariani, S., Fiebig, M., Koeberl, C., and Bice, D.M., 2019, Luminescence geochronology of Pleistocene slack-water deposits in the Frasassi hypogenic cave system, Italy, *in* Koeberl, C., and Bice, D.M., eds., 250 Million Years of Earth History in Central Italy: Celebrating 25 Years of the Geological Observatory of Coldigioco, v. 542, Geological Society of America, p. 411.

National Park Service, 2007, Digital geologic map of Great Basin National Park and vicinity, Nevada: National Park Service, U.S. Department of the Interior, online at https://irma.nps.gov/DataStore/Reference/Profile/1044849 (accessed December 2020).

Nevada Bureau of Mines and Geology, 2010, Site Description: Steptoe Valley: https://data.nbmg.unr.edu/Public/Geothermal/SiteDescriptions/SteptoeValley.pdf (accessed December 2020).

Onac, B.P., Veni, G., and White, W.B., 2001, Depositional environment for metatyuyamunite and related minerals from Caverns of Sonora, TX (USA): European Journal of Mineralogy, v. 13, p. 135-143, https://doi.org/10.1127/0935-1221/01/0013-0135

Osborne, R.A., 2004, The trouble with cupolas: Acta Carsologica, v. 33, n. 2, p. 10-36, https://speleogenesis.com/pdf/37OsborneCUPOLAS2004.PDF (accessed November 2020).

Palmer, A.N., 2007, Cave Geology: Cave Books, Dayton, OH, 453 p.

Palmer, A.N., 2013, Sulfuric acid caves: Morphology and evolution, *in* Shroder, J., and Frumkin, A. (eds.), Treatise on Geomorphology, v. 6, Karst Geomorphology: San Diego, Academic Press, p. 241–257, https://doi.org/10.1016/B978-0-12-374739-6.00133-0.

Palmer, A.N., and Palmer, M.V., 2000, Hydrochemical interpretation of cave patterns in the Guadalupe Mountains, New Mexico: Journal of Cave and Karst Studies, v. 62, p. 91-108.

Palmer, M.V., and Palmer, A.N., 2012, Petrographic and isotopic evidence for late-stage processes in sulfuric acid caves of the Guadalupe Mountains, New Mexico, USA: International Journal of Speleology, v. 41, p. 231-250, http://dx.doi.org/10.5038/1827-806X.41.2.10 (accessed November 2020).

Polyak, V.J., McIntosh, W.C., Guven, N., and Provencio, P., 1998, Age and origin of Carlsbad Cavern and related caves from $^{40}Ar/^{39}Ar$ of alunite: Science, v. 279, p. 1919-1922.

Polyak, V.J., and Mosch, C.J., 1995, Metatyuyamunite from Spider Cave, Carlsbad Caverns National Park, New Mexico: NSS Bulletin, v. 57, p. 85-90.

Polyak, V.J., and Provencio, P.P., 2001, By-product materials related to H_2S-H_2SO_4 influenced speleogenesis of Carlsbad, Lechuguilla, and other caves of the Guadalupe mountains, New Mexico, Journal of Cave and Karst Studies, v. 63, p. 23-32.

Prudic, D.E, Sweetkind, D.S., Jackson, T.L., Dotson, K.E., Plume, R.W., Hatch, C.E., and Halford, K.J. 2015, Evaluating connection of aquifers to springs and streams, Great Basin National Park and vicinity, Nevada: U.S. Geological Survey Professional Paper 1819, 188 p., http://dx.doi.org/10.3133/pp1819.

Richards, J.M., 2001, Lechuguilla Cave culvert access replacement: Canyons and Caves, no. 19, p. 6-9.

Rosales-Lagarde, L., 2013, Sulfidic karst springs and speleogenesis in the Sierra de Chiapas: Austin, Association for Mexican Cave Studies Bulletin 24, 79 p.

Rosales-Lagarde, L., Boston, P., Campbell, A., Hose, L., Axen, G., and Stafford, K.W., 2014, Hydrogeology of northern Sierra de Chiapas, Mexico: A conceptual model based on a geochemical characterization of sulfide-rich karst brackish springs: Hydrogeology Journal, v. 22, issue 6, p. 1447-1467.

Rossi, C., Lozano, R.P., Isanta, N., and Hellstrom, J., 2010, Manganese stromatolites in caves: El Soplao (Cantabria, Spain): Geology, v. 38, p. 1119-1122.

Rowley, P.D., Dixon, G.L., Mankinen, E.A., Pari, K.T., McPhee, D.K., McKee, E.H., Burns, A.G., Watrus, J.M., Ekren, E.B., Patrick, W.G., and Brandt, J.M., 2017, Geology and Geophysics of White Pine and Lincoln Counties, Nevada, and Adjacent Parts of Nevada and Utah: The Geologic Framework of Regional Groundwater Flow Systems: Nevada Bureau of Mines and Geology Report 56, Reno, Nevada, 146 p, https://pubs.nbmg.unr.edu/Geol-geophys-White-Pine-Lincoln-p/r056.htm (accessed December 2020).

Rozaire, C., 1964, The archeology at Lehman Caves National Monument: Nevada State Museum Report.

Sarbu, S.M., Kane, T.C., and Kinkle, B.K., 1996, A chemoautotrophically based cave ecosystem: Science**,** v. 272, p. 1953–1955.

Spilde, M.N., Boston, P.J., Northup, D.E. and Melim, L., 2008, New Mexico underground: Extreme geomicrobiology of caves in the southwest. Microscopy and Microanalysis, v. 14 (Suppl, 2). DOI: 10.1017/S1431927608085073

Stockli, D.F., 2005, Application of low-temperature thermochronometry to extensional tectonic settings: Reviews in Mineralogy and Geochemistry, v. 58, p. 411–448, doi:10.2138/rmg.2005.58.16.

White, W.B., 1988, Geomorphology and Hydrology of Karst Terrains: New York, Oxford University Press, 464 p.

Whitebread, D.H., 1969, Geologic map of the Wheeler Peak and Garrison quadrangles, Nevada and Utah: U.S. Geological Survey Miscellaneous Geologic Investigations Map I-478, scale 1:48,000, https://doi.org/10.3133/i578.

Winograd, I.J., and Thordarson, William, 1975, Hydrogeologic and hydrochemical framework south-central Great Basin, Nevada-California, with special reference to the Nevada Test Site: U.S. Geological Survey Professional Paper 712-C, 126 p., https://doi.org/10.3133/pp712C.

FIGURES

1. Location map for Cueva de Villa Luz, Mexico.
2. Location map for Frasassi Cave, Italy, created using Snazzy Maps (https://snazzymaps.com).
3. Location map for Carlsbad Caverns and Lechuguilla Cave in the Guadalupe Mountains of New Mexico.
4. Location map for east-central Nevada hypogenic caves visited on this field trip. Stop 5: Sacramento Pass; Stop 6: Lehman Caves; Stop 7: Burial Cave; Stop 8: Crystal Ball Cave; Stop 9: Pescio Cave; Stop 10: Discovery Cave; Stop 11: Old Mans Cave.
5. Simplified map of Cueva de Villa Luz with stop locations. Based on a detailed map by Bob Richards in Hose et al. (2000).
6. Sulfur folia on walls near the Yellow Roses subterranean spring.
7. Schematic cross-section of the Yellow Roses room.
8. Group of sulfuric acid-dripping snottites suspended from selenite crystals in Cueva de Villa Luz. Photo by Art Palmer and Peg Palmer.

9. Schematic cross-section of the Sala Grande in Cueva de Villa Luz.
10. Pool Room just upstream from the Main Entrance. Fish in the cave swim near the surface of the pool, where there is more oxygen available. Photo by Stephen Alvarez.
11. Schematic cross-section of the Pool Room in Cueva de Villa Luz.
12. Biovermiculation on limestone bedrock wall in Cueva de Villa Luz.
13. Map of the Grotta Grande del Vento-Grotta del Fiume (GGV-GdF) cave complex, showing stop locations for this virtual field trip. Base map after Mariani et al. (2007), and courtesy of the Gruppo Speleologico CAI di Fabriano. GM-GF is located approximately 500 m to the northeast of GGV, just off the northern edge of the map.
14. a. Image on the left of white stream biofilms. The photograph was taken during a period with slower streamflow and the white mats are primarily sediment-water interface biofilms formed by *Beggiatoa* spp.; b. Biovermiculations on the right at Pozzo dei Cristalli. The white wall deposits are microcrystalline gypsum crusts, with a carabiner for scale.
15. General schematic of microbial communities at the Frasassi water table. Hydrogen sulfide (H_2S) supports microbial biofilms in the streams and on the walls, and gypsum corrosion residues form above the water table from the reaction between sulfuric acid and limestone. Gypsum wall crusts eventually detach and accumulate on the floor, where they can form large deposits that may persist for long periods of time, and may eventually end up as “glaciers” like those in the older cave levels. (From Jones and Northup, in review).
16. A large gypsum deposit in Sala della Sabbia. Zoë Havlena for scale. The vertical grooves visible on the gypsum surface are drip holes created by fresh waters.
17. Locations of stops in Carlsbad Cavern.
18. Trays on the wall near the place where the tourist trail enters the Big Room (Stop 3.2).

19. Coralloid-encrusted drip tubes near Fairyland in the Big Room (Stop 3.3).
20. Illustration of a gypsum mass perforated by dripping water to form drip tubes.
21. Drip tube in gypsum block near Jumping Off Place, Big Room (Stop 3.4).
22. Gypsum block in alcove near Mirror Lake, Big Room (Stop 3.5). Note gypsum mass and pseudoscallops in alcove.
23. Solution rills in Left Hand Tunnel (Stop 3.6). Photo by Art Palmer and Peg Palmer.
24. Map of Lechuguilla Cave showing locations of field trip stops.
25. Massive gypsum modified by dripping water in Glacier Bay. This is the first occurrence of massive gypsum encountered when traveling into Lechuguilla Cave.
26. Speleogenetic features including bedrock solution pendants and acid pool basin, Emperor's Throne Room, Lechuguilla Cave. Photo by David Harris, Harris Photographic.
27. Acid pool basin, Bryce Canyon area, Far East branch, Lechuguilla Cave. Photo by Kathryn Sisson DuChene.
28. Mostly dissolved gypsum mass (right side of photo) and coralloid-encrusted drip tube (lower left corner of photo) near High Hopes, Southern Branch, Lechuguilla Cave. Note that there are two sets of drip tubes. Photo by Kathryn Sisson DuChene.
29. Partly dissolved gypsum mass beneath trays in Never Never Land, Lechuguilla Cave. Photo by Art Fortini.
30. Stratigraphic section for the Snake Range of Nevada.
31. Map of Lehman Caves with stop locations. Cartography by Shane Fryer and Cynthia Walck. Geology shown in the profile represents earlier understanding. Today, we know that quartzite overlies much of the northern portions of the cave and the foliation of the marble typically dips nearly vertical.

32. Upper plate of a large cave shield in the Gothic Palace of Lehman Caves. Note the horizontal calcite ridges, which we interpret as paleo-waterlines or mini-folia that formed when the lower plate was still intact and capillary water rose and receded within the crack between the two plates. Photo by Tom Wilson.
33. Numerous vertical holes in a calcite flowstone slope at Stop 6.3 appear to have been drilled by water drips from the stalactites overhead. Flagging tape mark the holes. The deepest is 42-cm deep.
34. Pseudoscallops, condensation corrosion, and other "speleogens" (bedrock shapes formed by dissolution processes) at Stop 6.3. Photo by Tom Wilson.
35. Talus Room in in the northwest part of Lehman Caves. The entrance to the Gypsum Annex is along the left-side wall with historical graffiti. Lower left of white lines point to people for scale. Photo by Dave Bunnell.
36. Geological map of surface over Lehman Caves. The black shadow shows the sub-surface outline of Lehman Caves below.
37. Undercut passage wall at the water level in an ancient acid pool basin at Stop 6.5 in the Gypsum Annex of Lehman Caves. Note cuspate indentations on downward-facing surface and rills on the wall above the overhang. Photo by Dave Bunnell.
38. Trays in a constricted part of the passage at Stop 6.6 in Gypsum Annex. White lines highlight the flat, but not necessarily horizontal, bottoms of some trays. Photo by Dave Bunnell.
39. Several low mounds resembling stalagmites with apparent drip holes are clustered in the northern Talus Room under matching stalactites. They lack the coral-encrustation of the encrusted drip tubes we see elsewhere in the cave.

40. Acidic condensation and rock-eating microbes have caused extensive corrosion of the marble bedrock and calcite speleothems throughout the cave. At Stop 6-14, turnip speleothems and the bedrock on the ceiling have been extensively corroded. Photo by Tom Wilson.
41. Shadow maps of east-central Nevada caves. a.) Burial Cave. Based on map by Tom Gilleland; b.) Crystal Ball Cave. Based on map by Dale Green; c.) Pescio Cave. Based on map by Shawn Thomas; d.) Discovery Cave. Based on map by Bern Szukalski; e.) Old Mans Cave. Based on map by Alvin McLane.
42. Folia in the lower passage of Burial Cave. Photo by Tom Strong.
43. Nailhead calcite spar forms a "crystal ball" in Crystal Ball Cave, Utah.
44. Encrusted drip tubes in the Coral Forest of Pescio Cave. The depth of the hole from the top of the encrustation is 45 cm and the external diameter is 10 x 15 cm. The internal diameter is about 3 x 8 cm. The tape measure shows centimeters. Note the rill-like development and bisected large drip tube immediately downslope. Note the heavily corroded mammillaries in the upper right of the photo on the left.
45. Folia in Discovery Cave dipping 6^{o} towards 270^{o} must have formed during uplift of this part of the northern Snake Range.
46. Hypogenic boneyard features. a.Keyhole passage at stop 11.1 follows a floor crevice, which could have been a source of ascending, acidic waters, common to hypogenic caves. The sides of the floor channel are lined with white precipitate, visible along the right side of the image, with cupolas visible overhead. b. Examples of Vent Room boneyard speleogens and a stratification line marking the top of sub-aerial cave coral deposition in the center of the photo, which was taken by Dave Bunnell.

47. Coral pipes on the slope of a stalagmite at Stop 11-3. a. Note that the morphology of the slope below the coral pipes is similar to the morphology of massive gypsum deposits in sulfuric acid speleogenesis caves (Fig. 3-4, 3.5, 3.6, 4.3); b. Close-up of coral pipes show coralloid caps at the top of the hoodoo-like structures. Photo by Dave Bunnell.

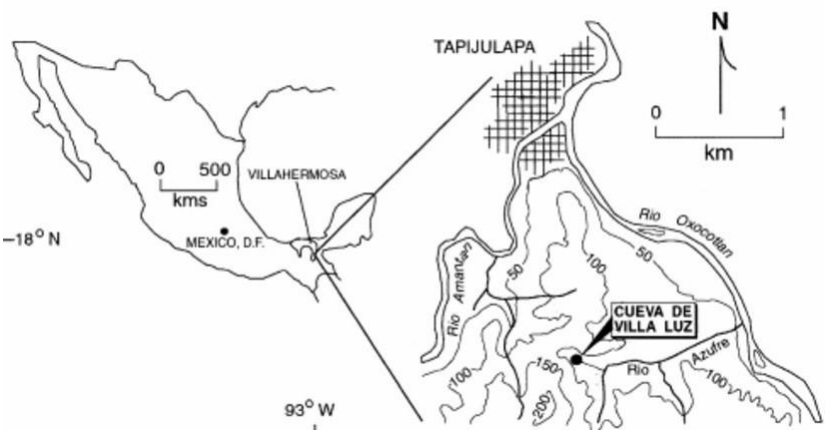

Figure 1

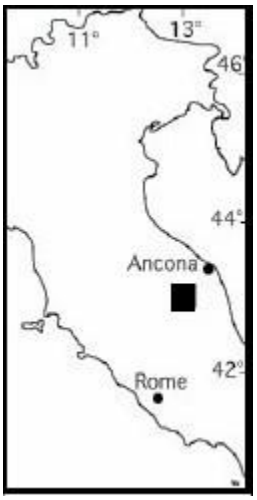

Figure 2

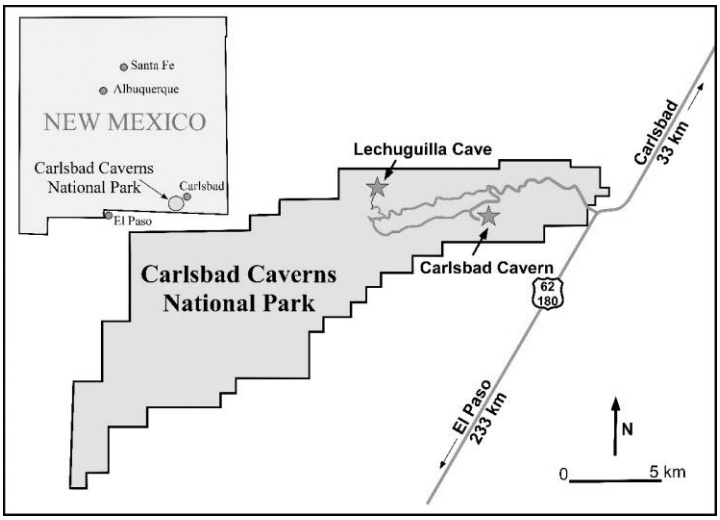

Figure 3

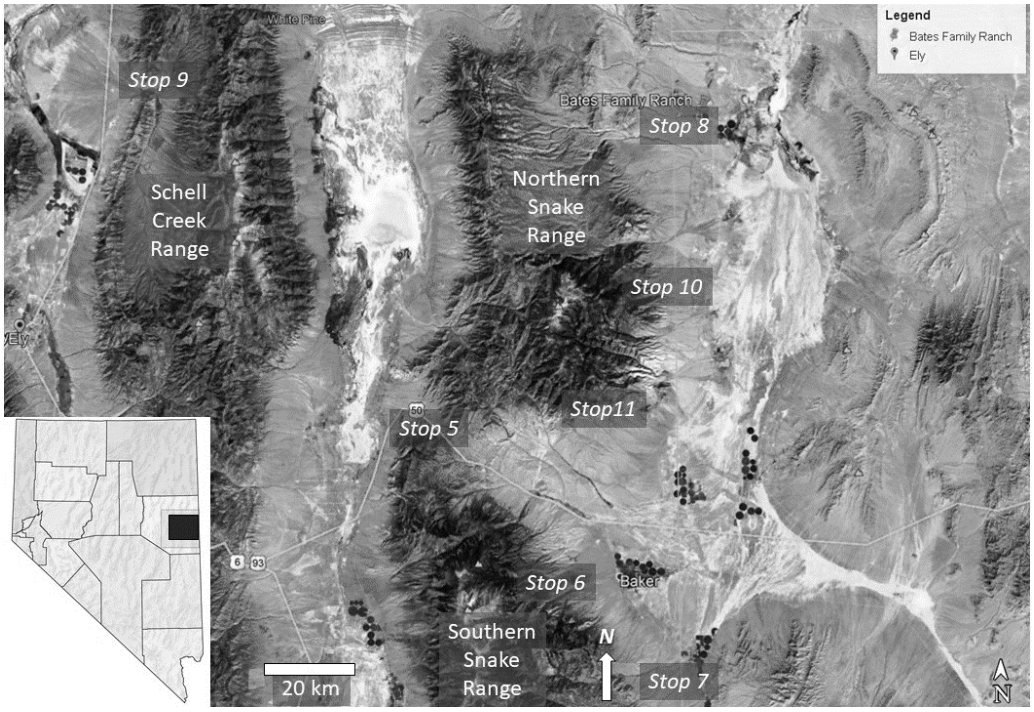

Figure 4

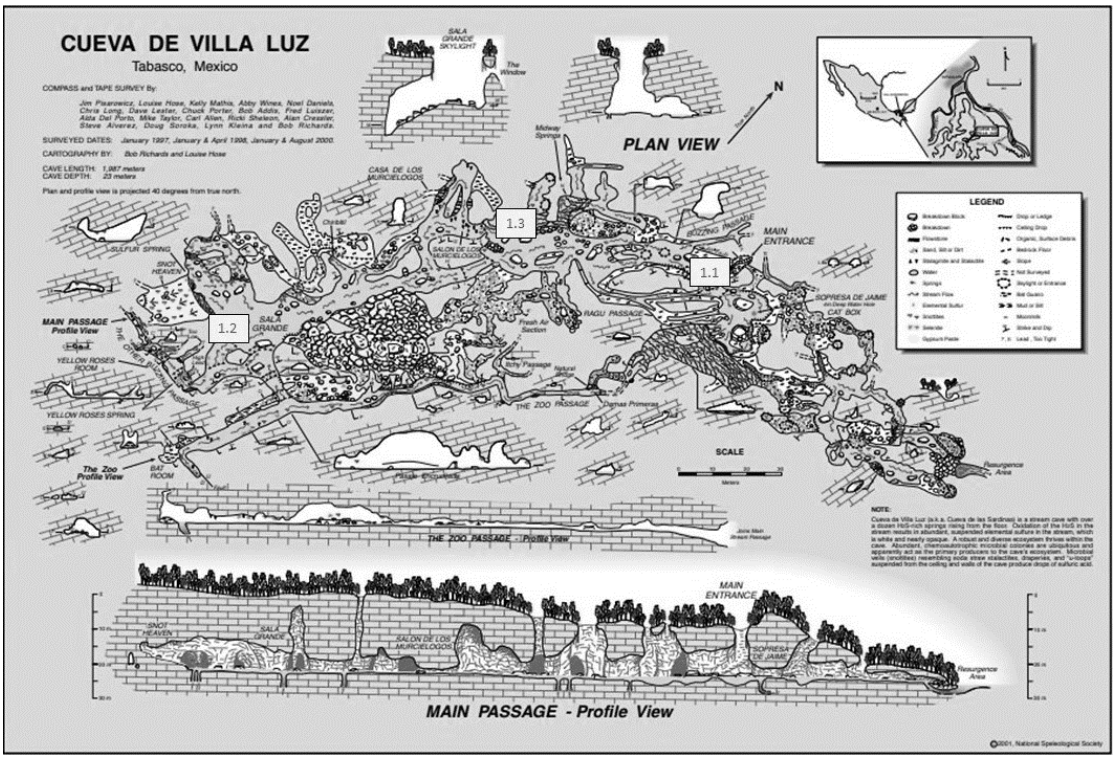

Figure 5

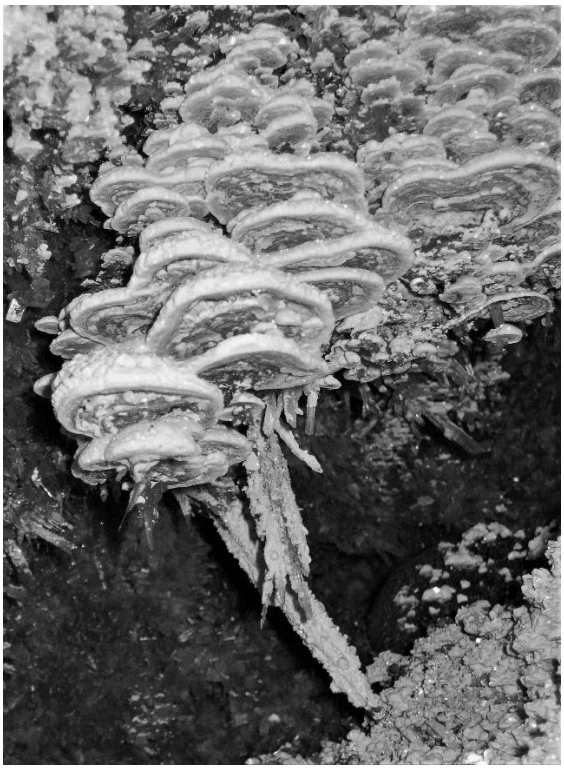

Figure 6

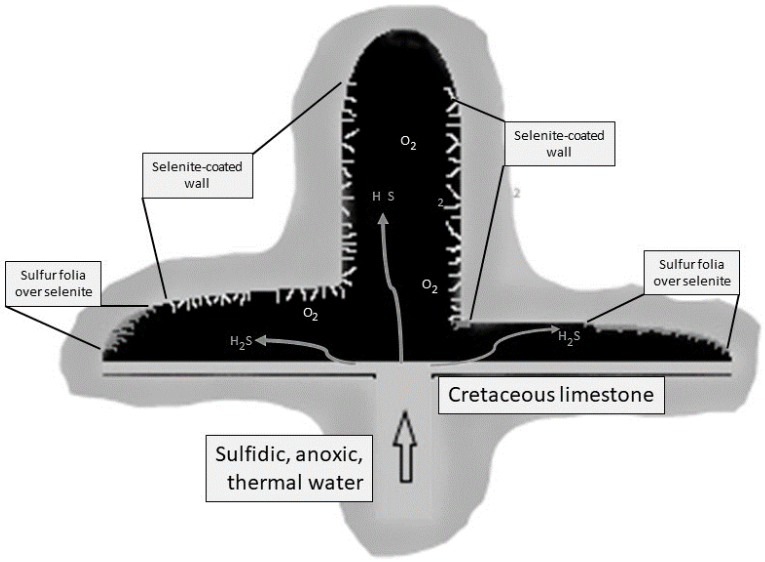

Figure 7

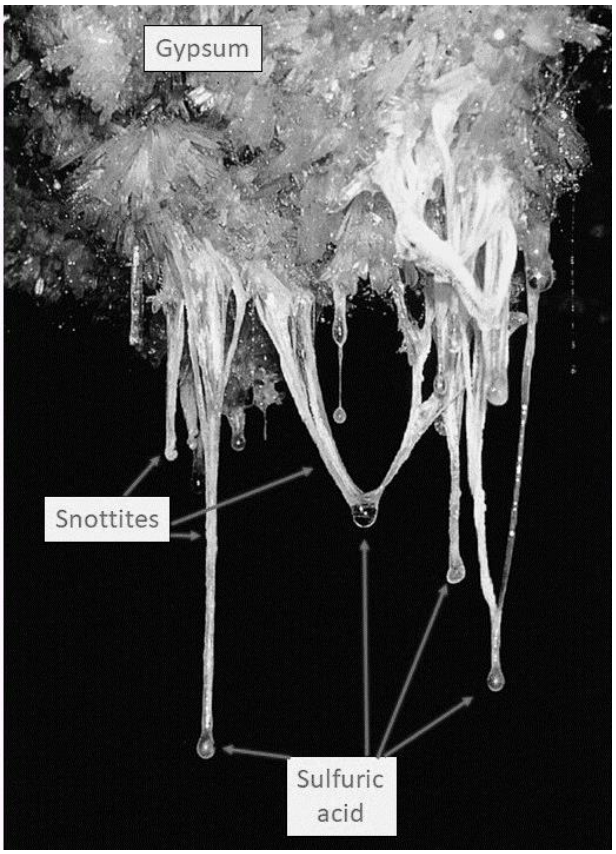

Figure 8

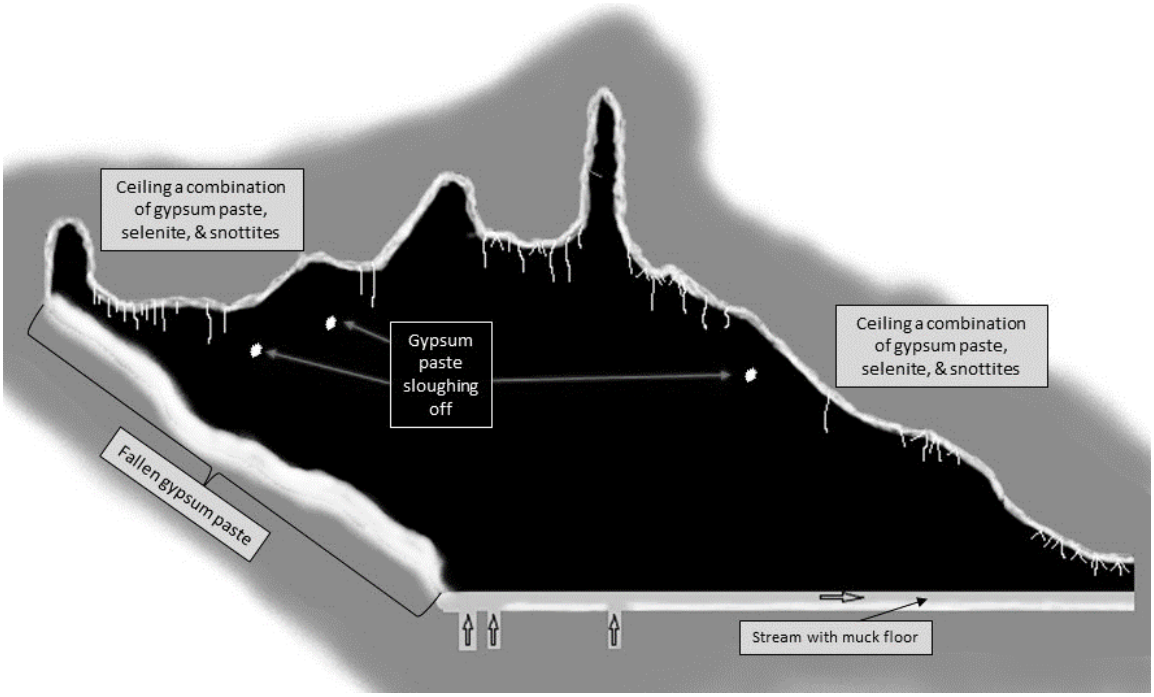

Figure 9

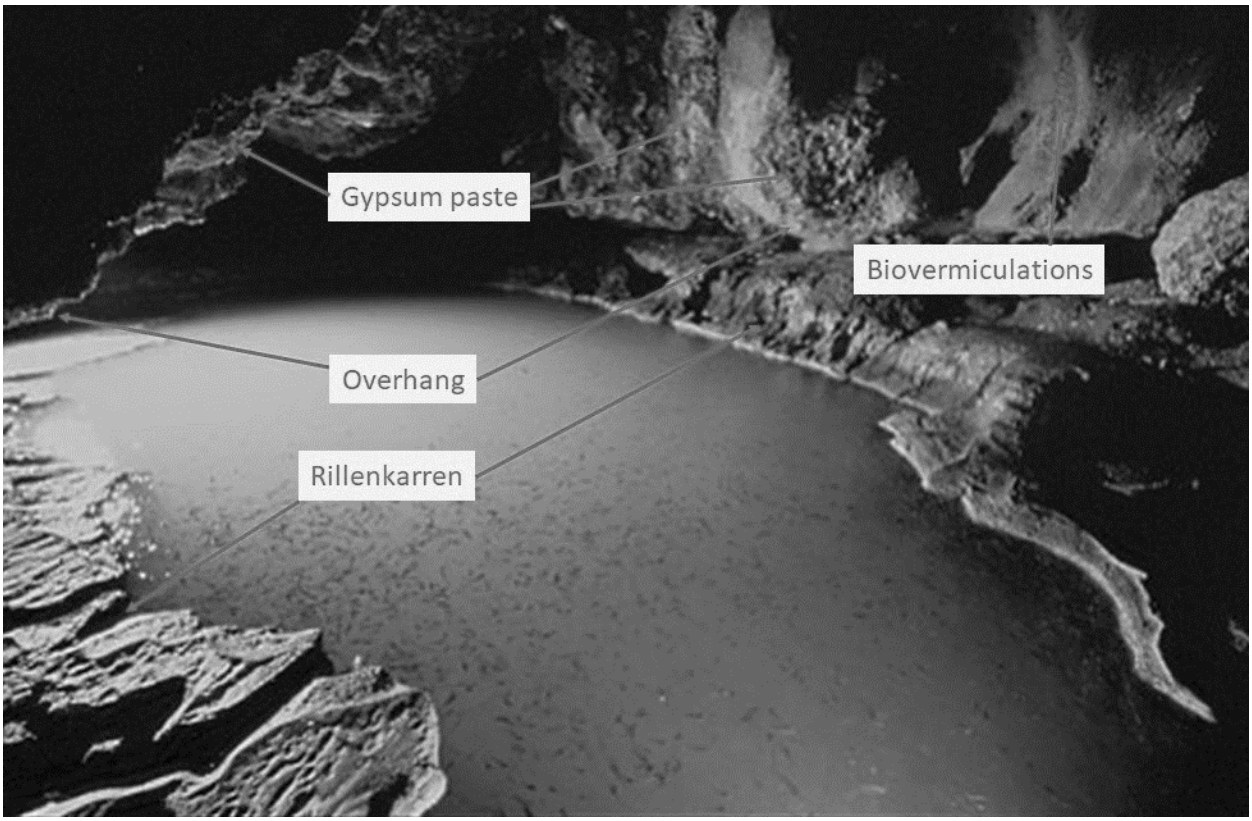

Figure 10

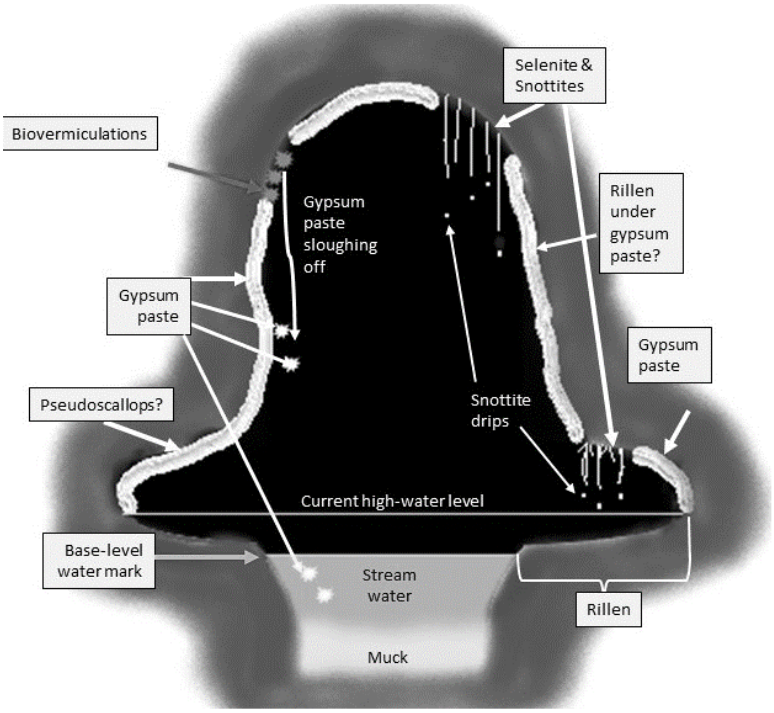

Figure 11

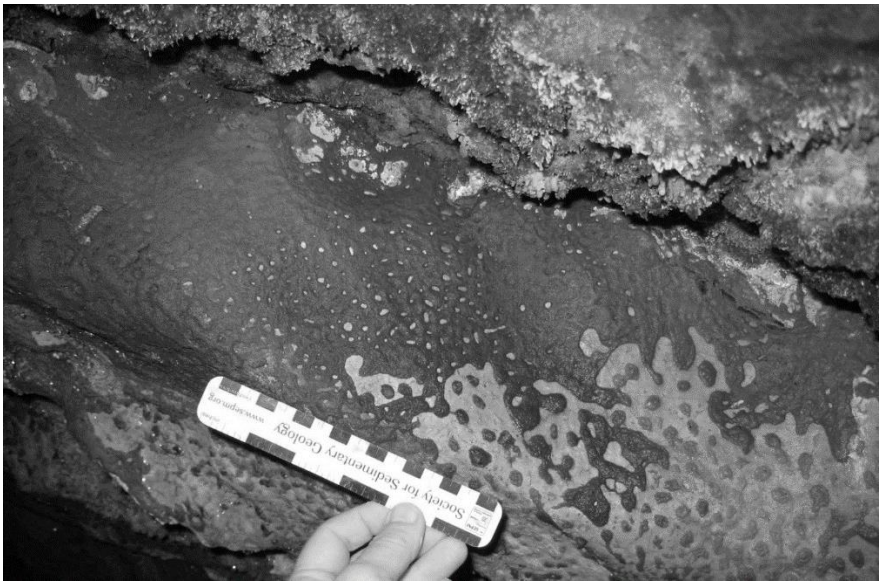

Figure 12

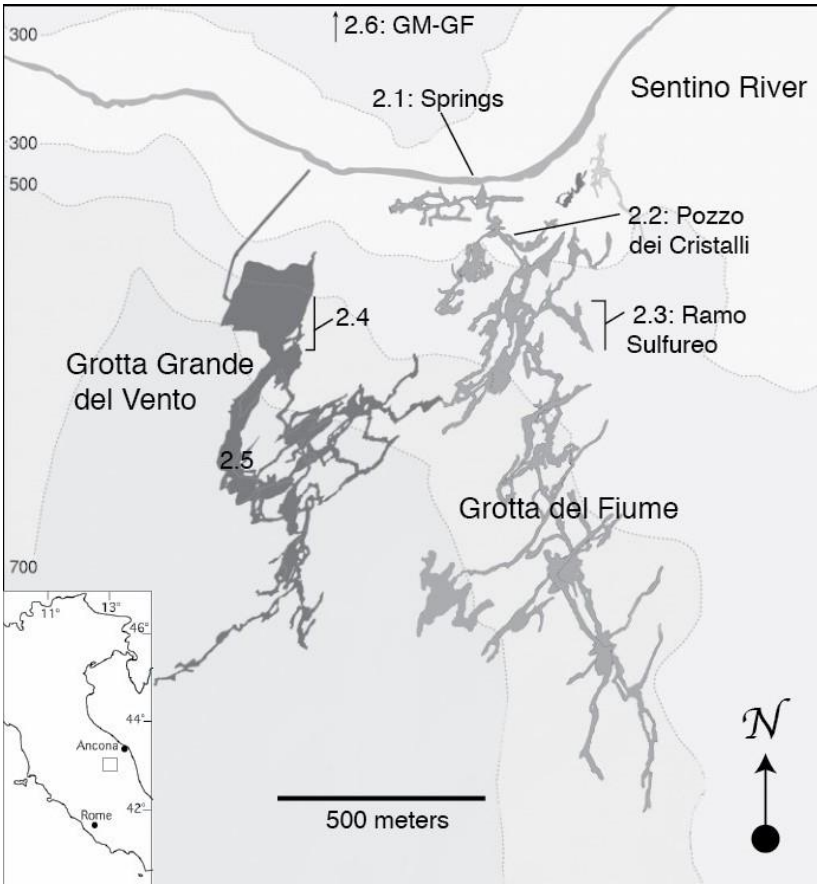

Figure 13

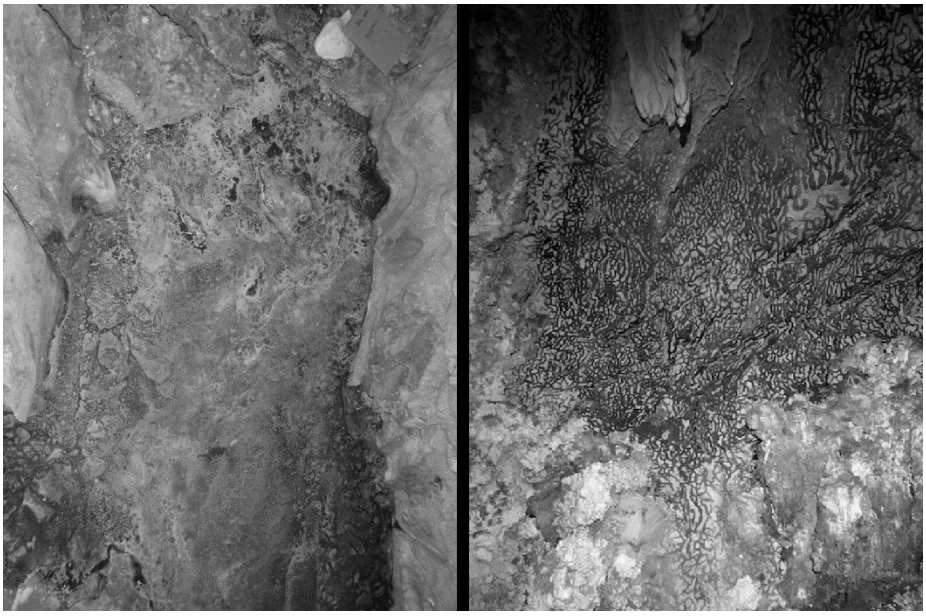

Figure 14

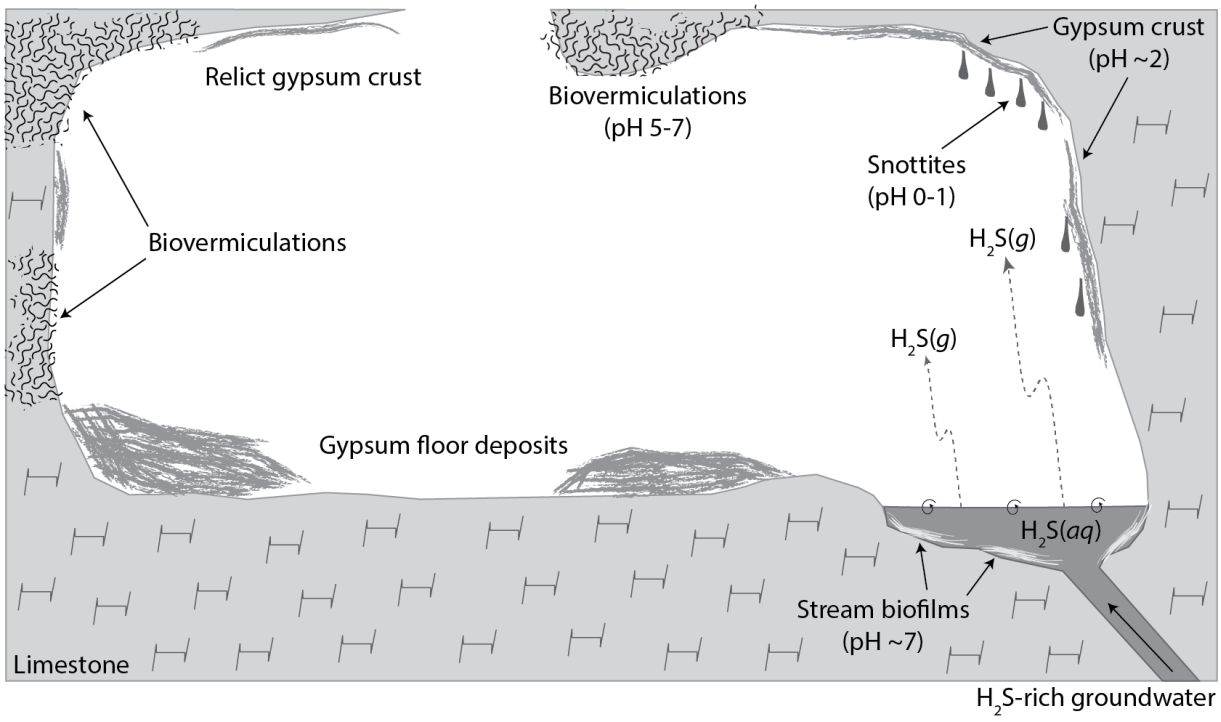

Figure 15

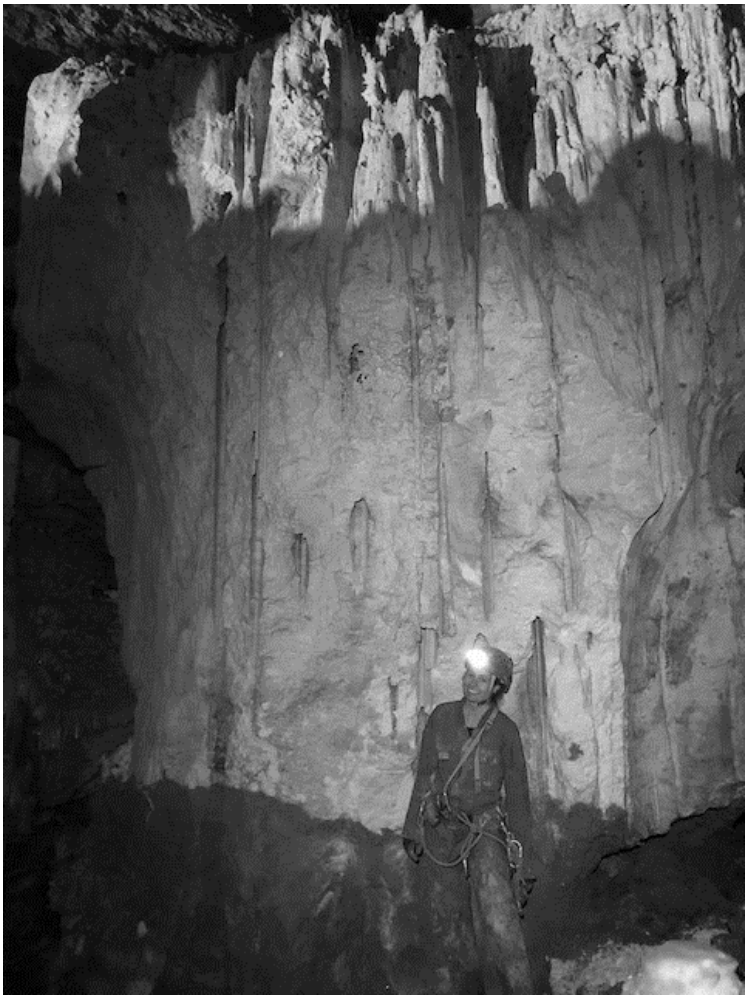

Figure 16

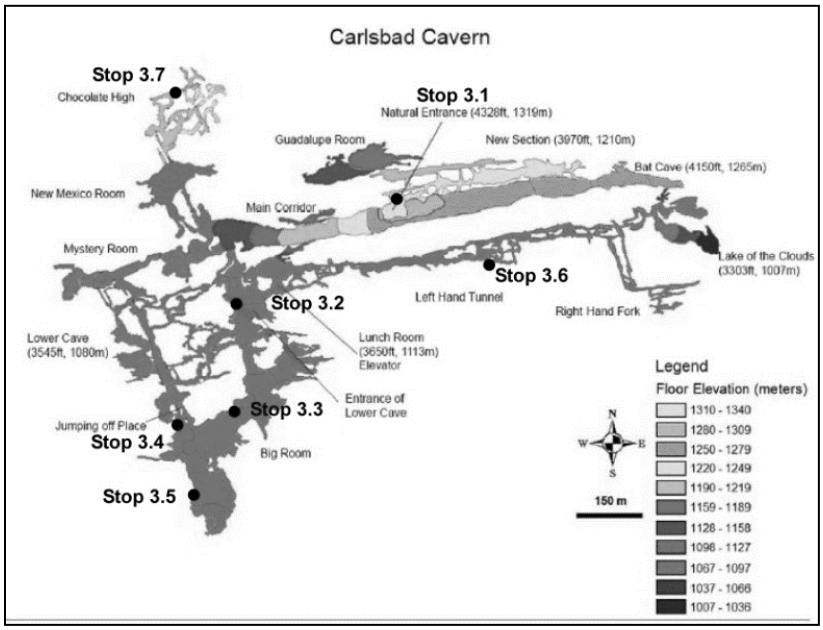

Figure 17

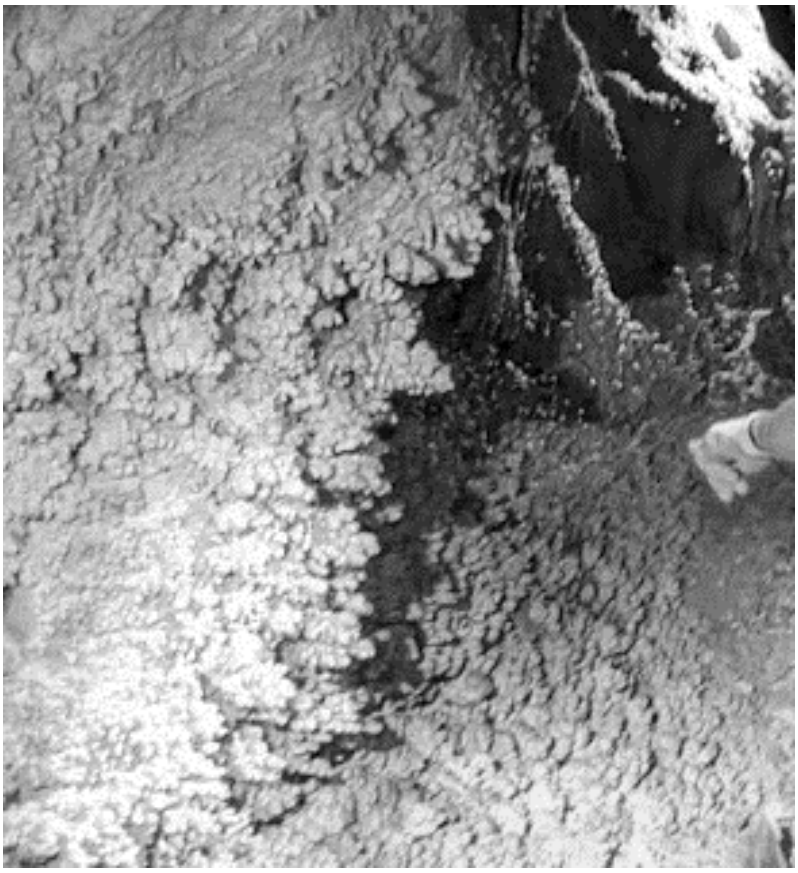
Figure 18

Figure 19

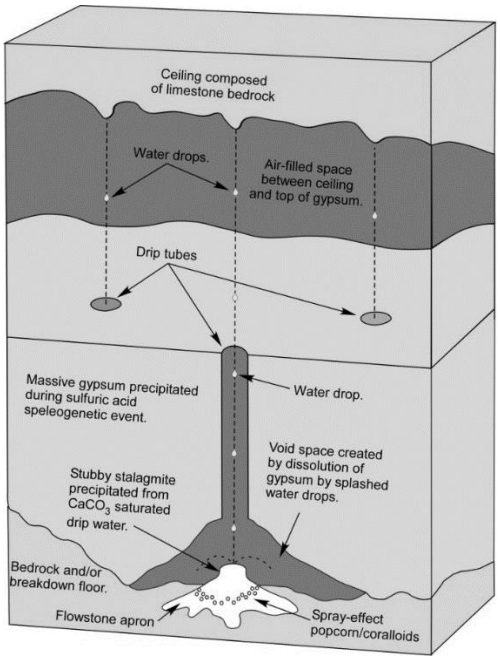

Figure 20

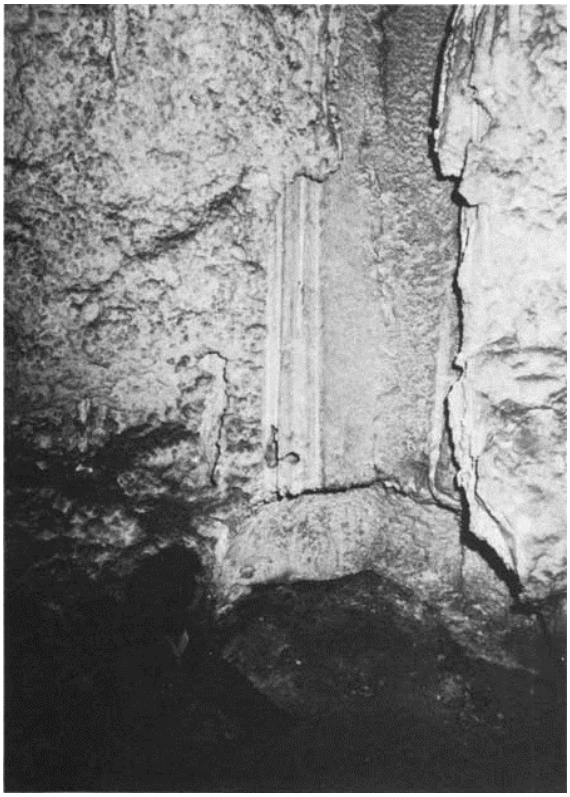

Figure 21

Figure 22

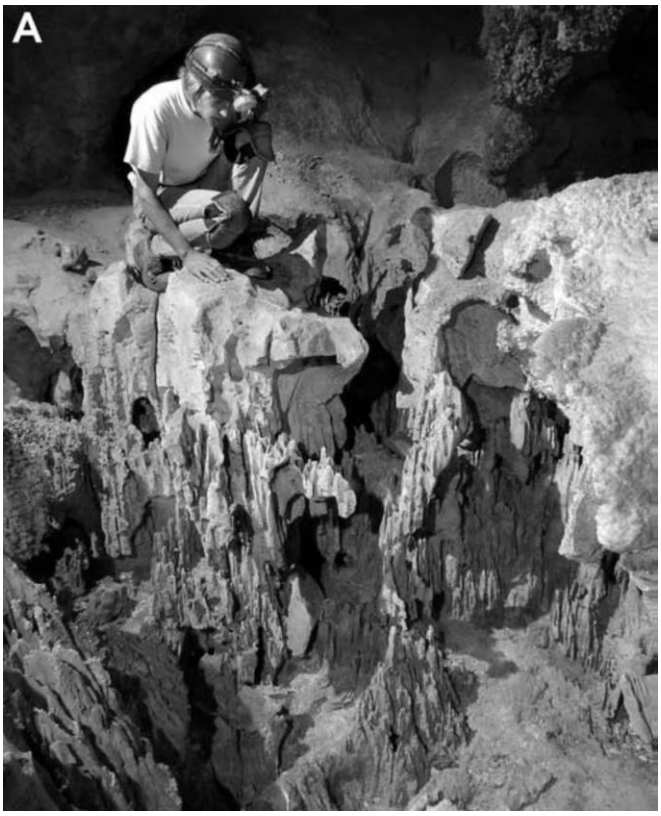

Figure 23

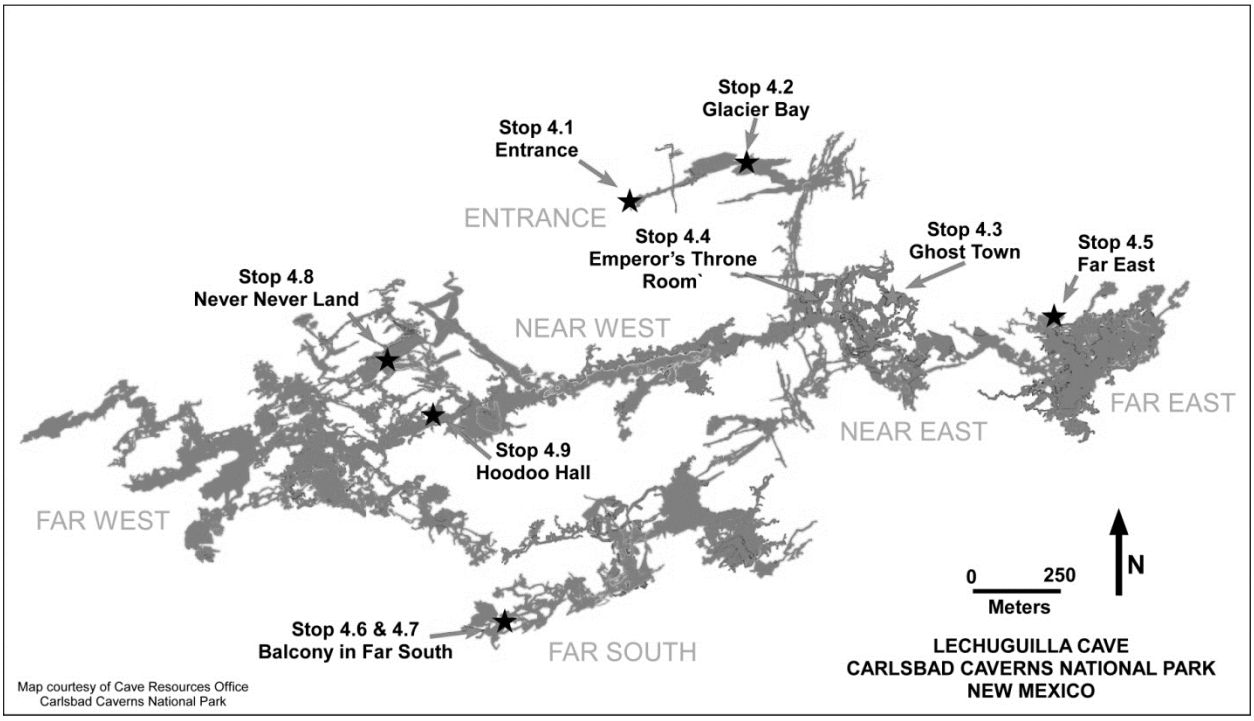

Figure 24


Figure 25

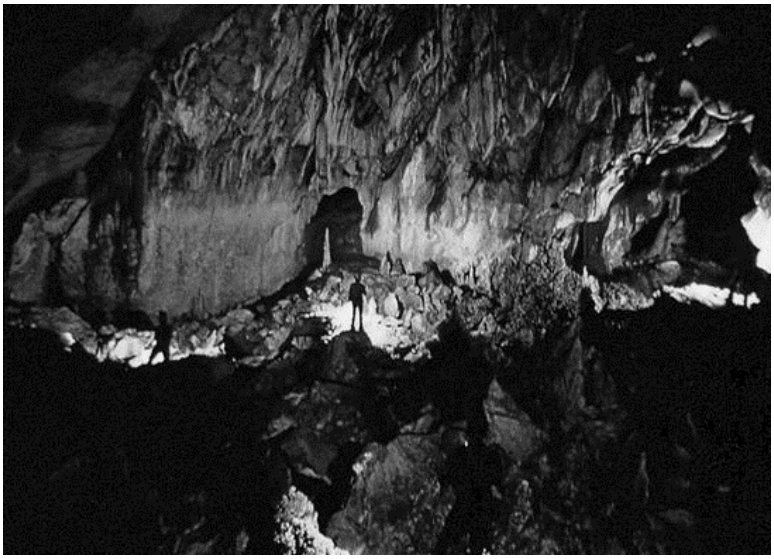

Figure 26

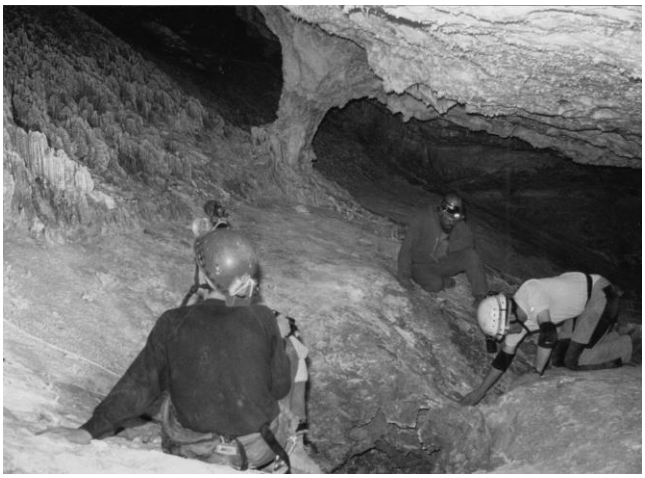

Figure 27

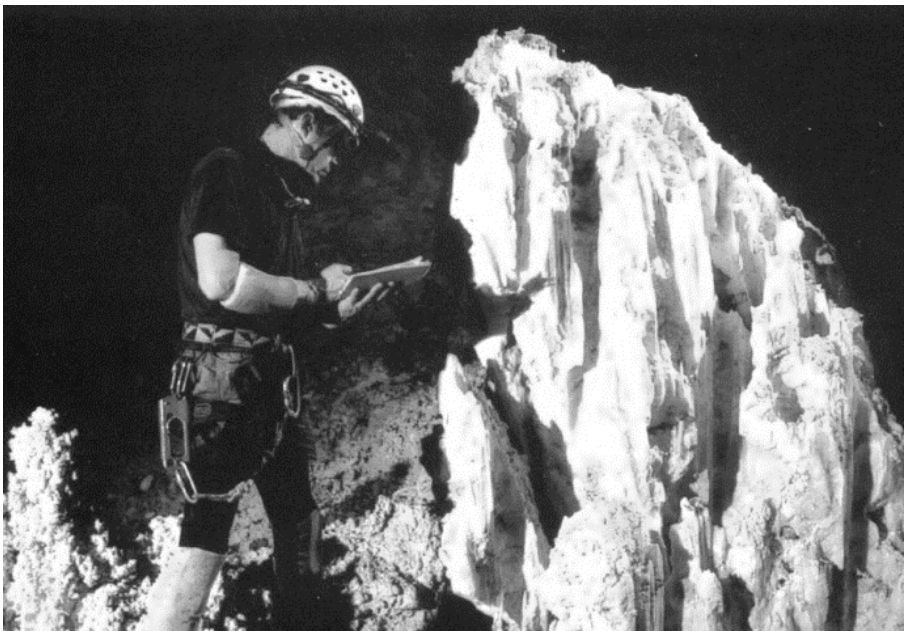

Figure 28

Figure 29

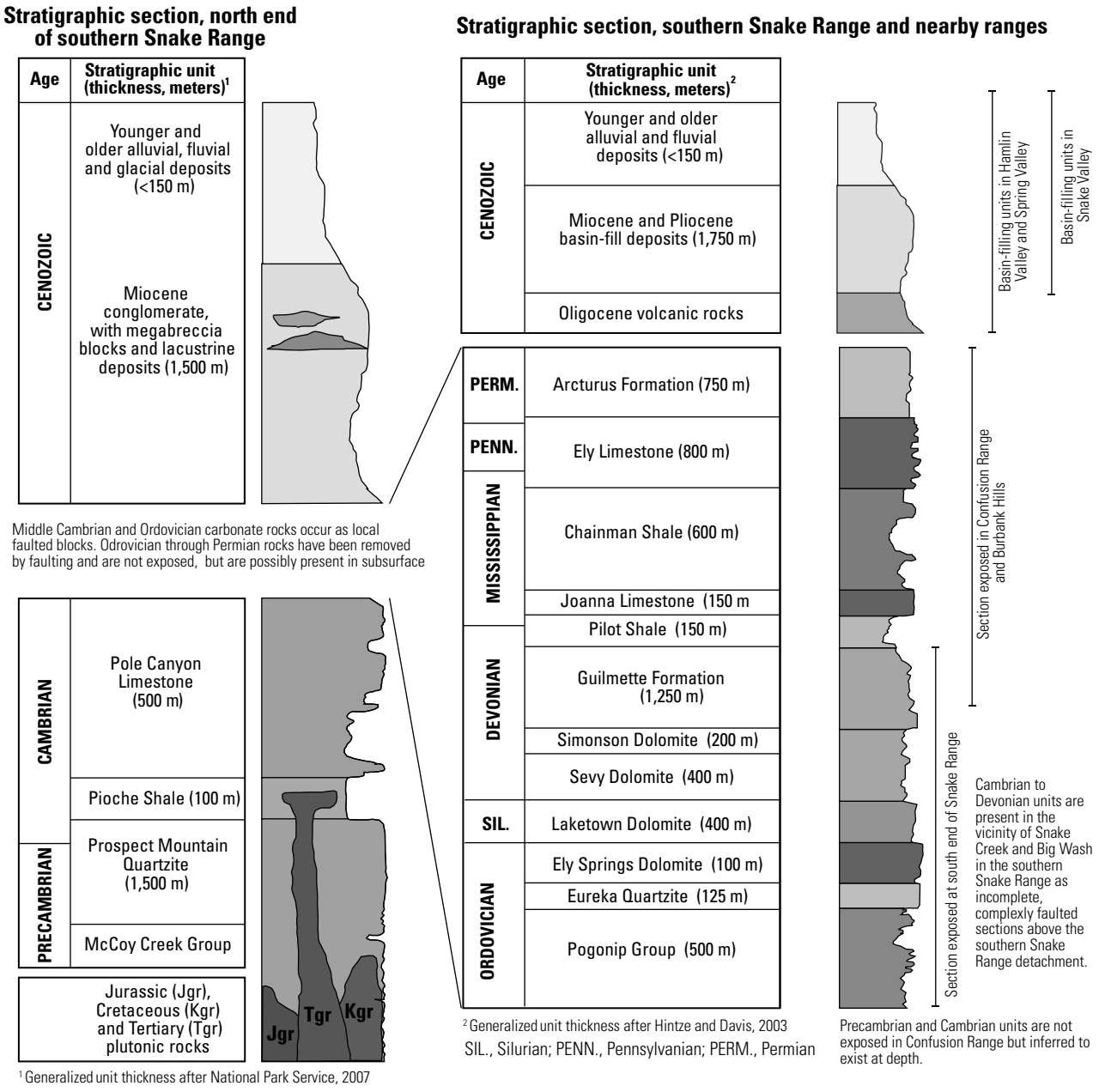
Stratigraphic section, north end of southern Snake Range
Age
Stratigraphic unit (thickness, meters)[1]
CENOZOIC
Younger and older alluvial, fluvial and glacial deposits (<150 m)
Miocene conglomerate, with megabreccia blocks and lacustrine deposits (1,500 m)
Middle Cambrian and Ordovician carbonate rocks occur as local faulted blocks. Odrovician through Permian rocks have been removed by faulting and are not exposed, but are possibly present in subsurface
CAMBRIAN
Pole Canyon Limestone (500 m)
Pioche Shale (100 m)
PRECAMBRIAN
Prospect Mountain Quartzite (1,500 m)
McCoy Creek Group
Jurassic (Jgr), Cretaceous (Kgr) and Tertiary (Tgr) plutonic rocks
Jgr
Tgr
Kgr
[1] Generalized unit thickness after National Park Service, 2007
Stratigraphic section, southern Snake Range and nearby ranges
Age
Stratigraphic unit (thickness, meters)[2]
CENOZOIC
Younger and older alluvial and fluvial deposits (<150 m)
Miocene and Pliocene basin-fill deposits (1,750 m)
Oligocene volcanic rocks
PERM.
Arcturus Formation (750 m)
PENN.
Ely Limestone (800 m)
MISSISSIPPIAN
Chainman Shale (600 m)
Joanna Limestone (150 m
DEVONIAN
Pilot Shale (150 m)
Guilmette Formation (1,250 m)
Simonson Dolomite (200 m)
Sevy Dolomite (400 m)
SIL.
Laketown Dolomite (400 m)
ORDOVICIAN
Ely Springs Dolomite (100 m)
Eureka Quartzite (125 m)
Pogonip Group (500 m)
[2] Generalized unit thickness after Hintze and Davis, 2003
SIL., Silurian; PENN., Pennsylvanian; PERM., Permian
Basin-filling units in Hamlin Valley and Spring Valley
Basin-filling units in Snake Valley
Section exposed in Confusion Range and Burbank Hills
Section exposed at south end of Snake Range
Cambrian to Devonian units are present in the vicinity of Snake Creek and Big Wash in the southern Snake Range as incomplete, complexly faulted sections above the southern Snake Range detachment.
Precambrian and Cambrian units are not exposed in Confusion Range but inferred to exist at depth.

Figure 30

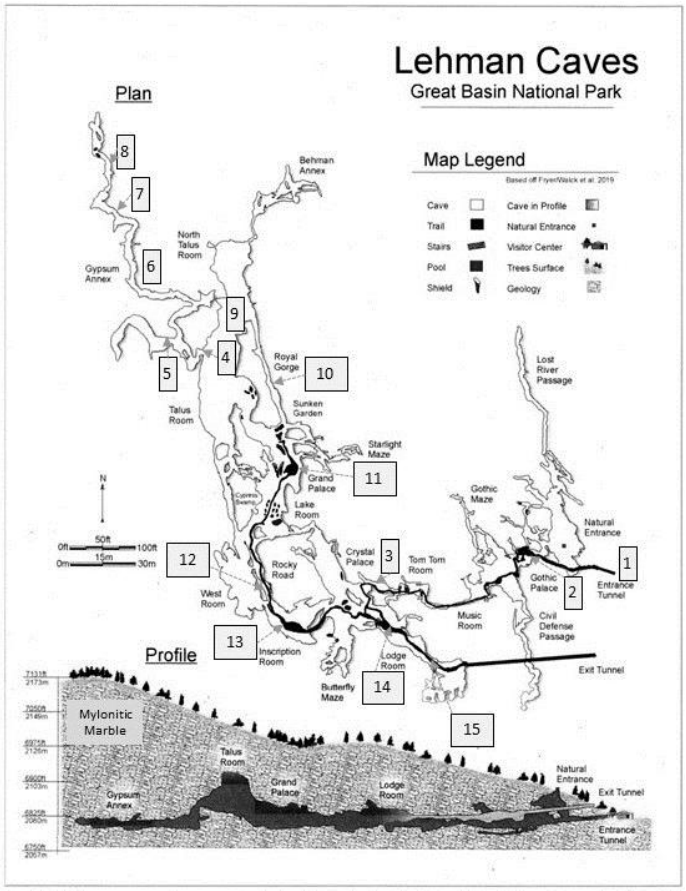

Figure 31

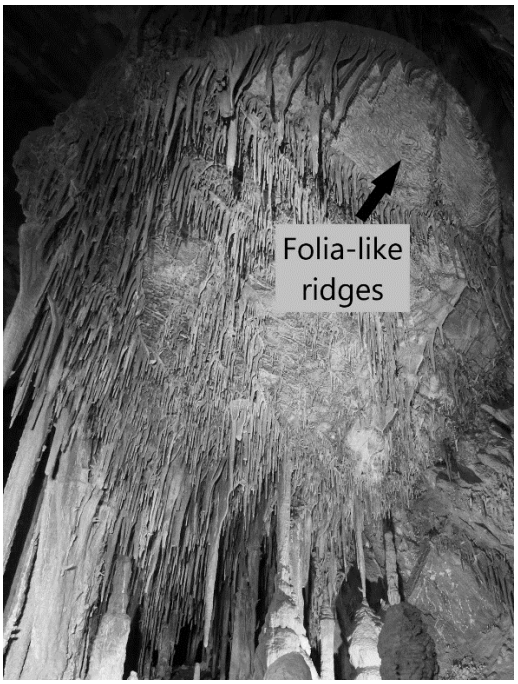

Figure 32

Figure 33

Figure 34

Figure 35

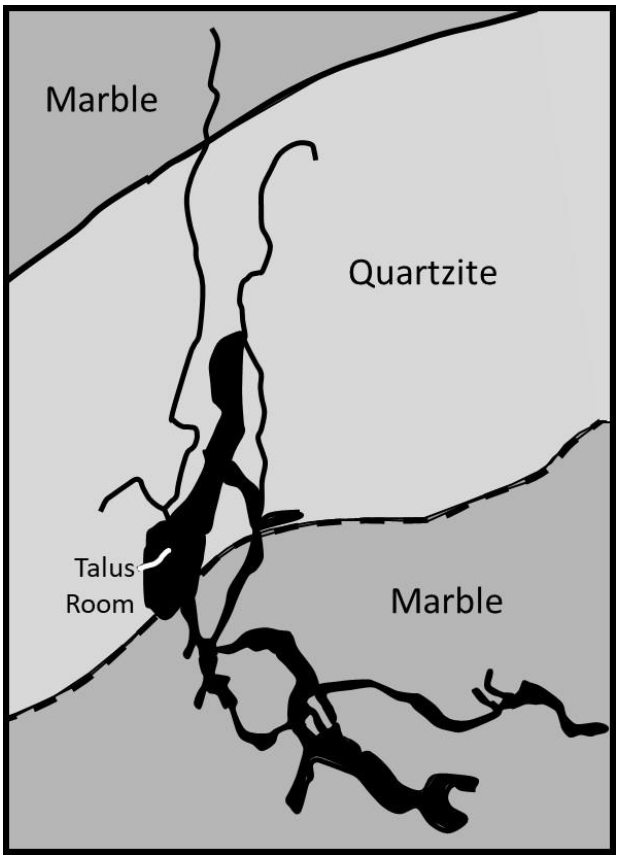

Figure 36

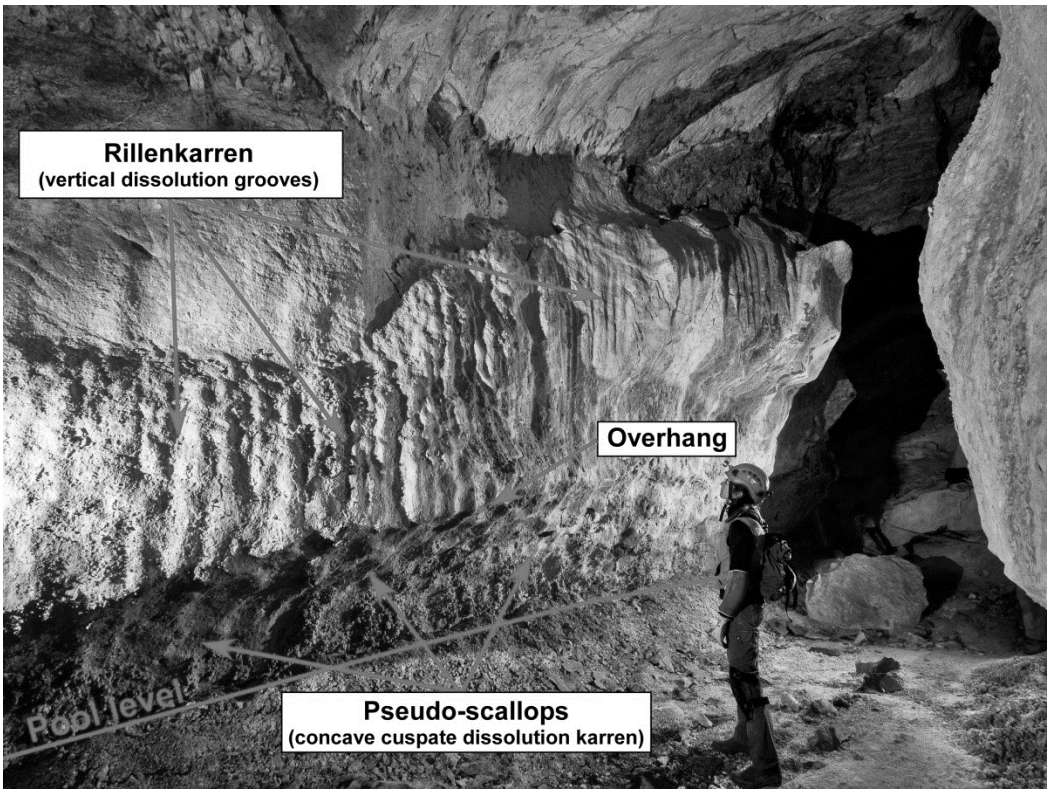

Figure 37

Figure 38

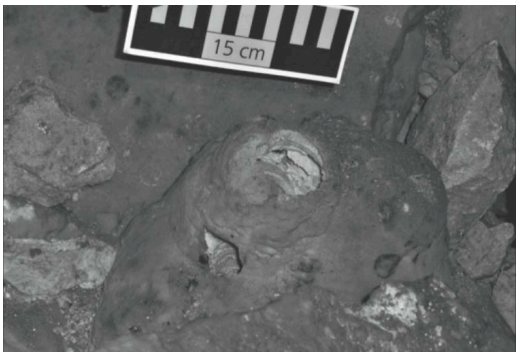

Figure 39

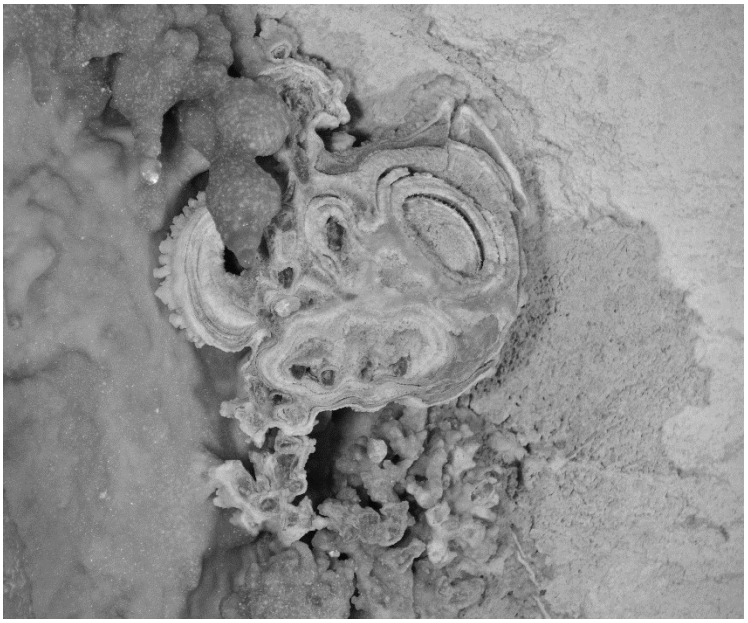

Figure 40

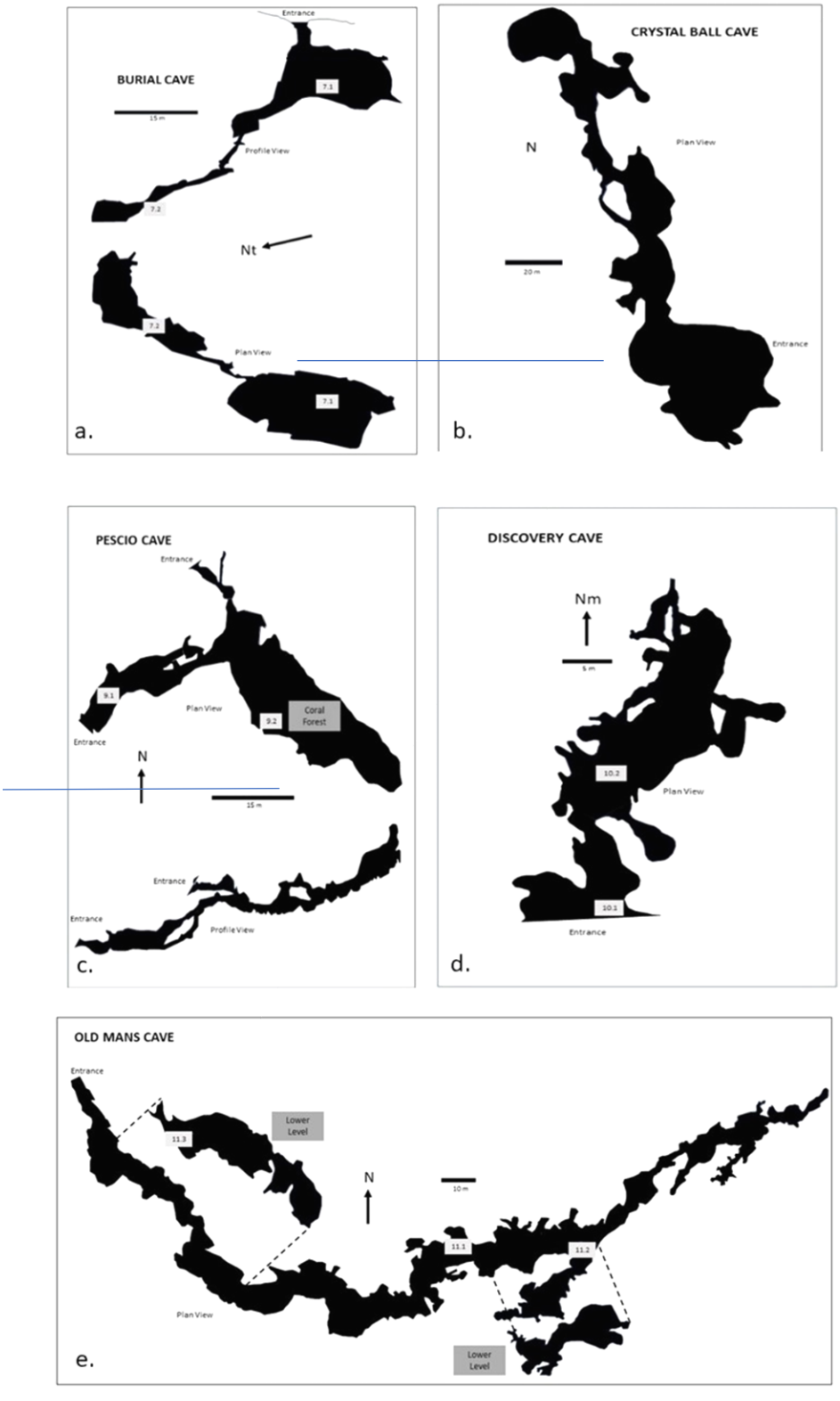
BURIAL CAVE
Entrance
7.1
15 m
Profile View
7.2
Nt
7.2
Plan View
7.1
a.
CRYSTAL BALL CAVE
N
Plan View
20 m
Entrance
b.
PESCIO CAVE
Entrance
9.1
Plan View
9.2
Coral Forest
Entrance
N
15 m
Entrance
Entrance
Profile View
c.
DISCOVERY CAVE
Nm
5 m
10.2
Plan View
10.1
Entrance
d.
OLD MANS CAVE
Entrance
11.3
Lower Level
N
10 m
11.1
11.2
Plan View
Lower Level
e.

Figure 41

Figure 42

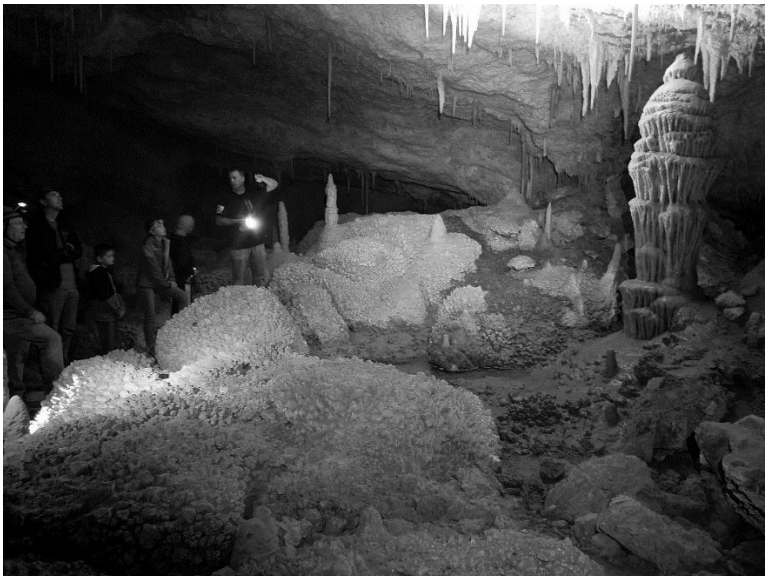

Figure 43

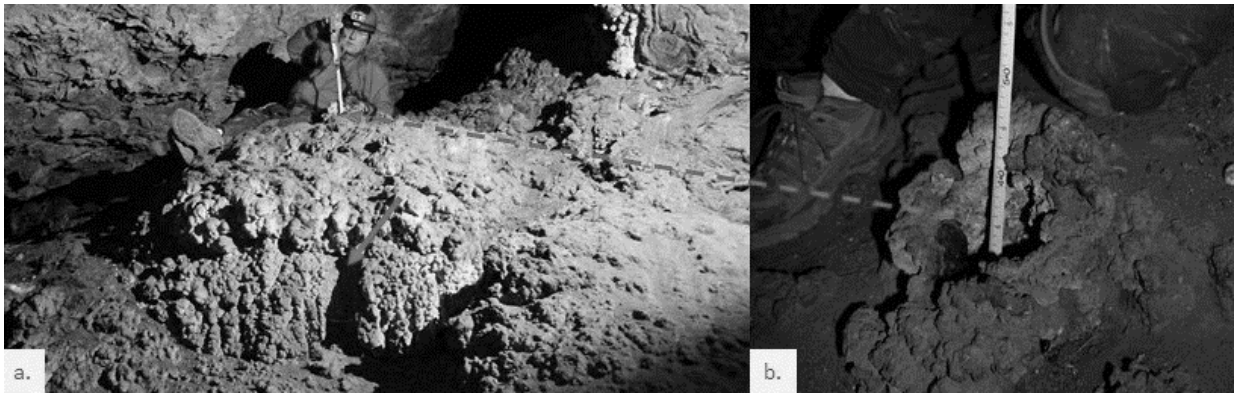

Figure 44

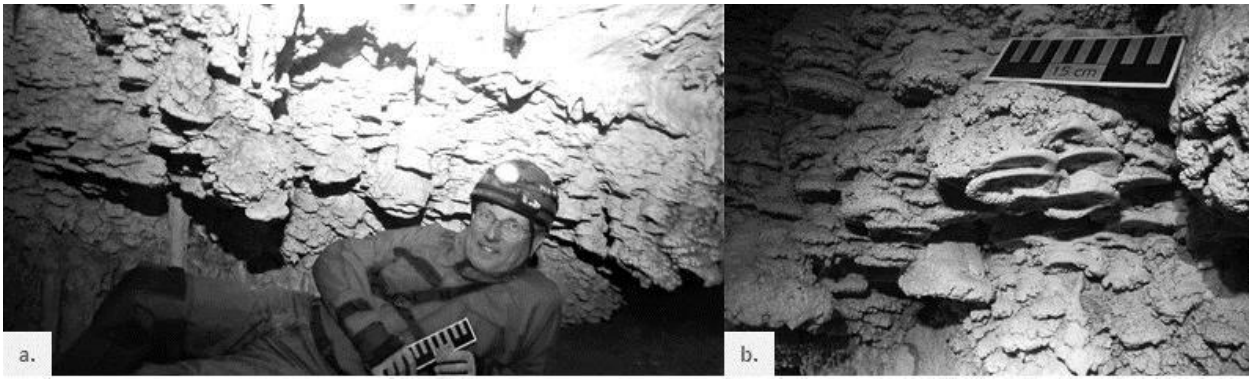

Figure 45

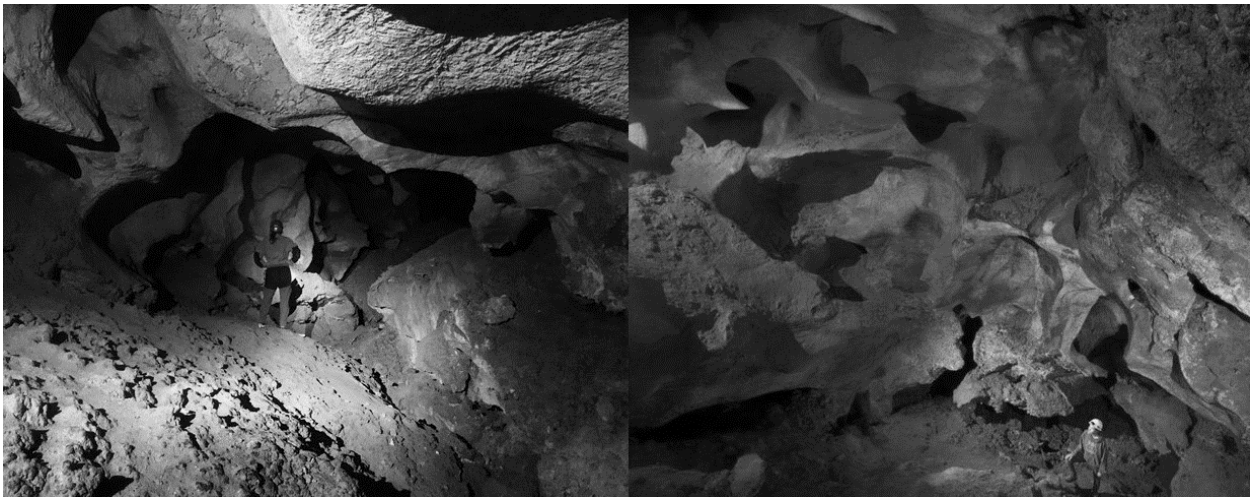

Figure 46

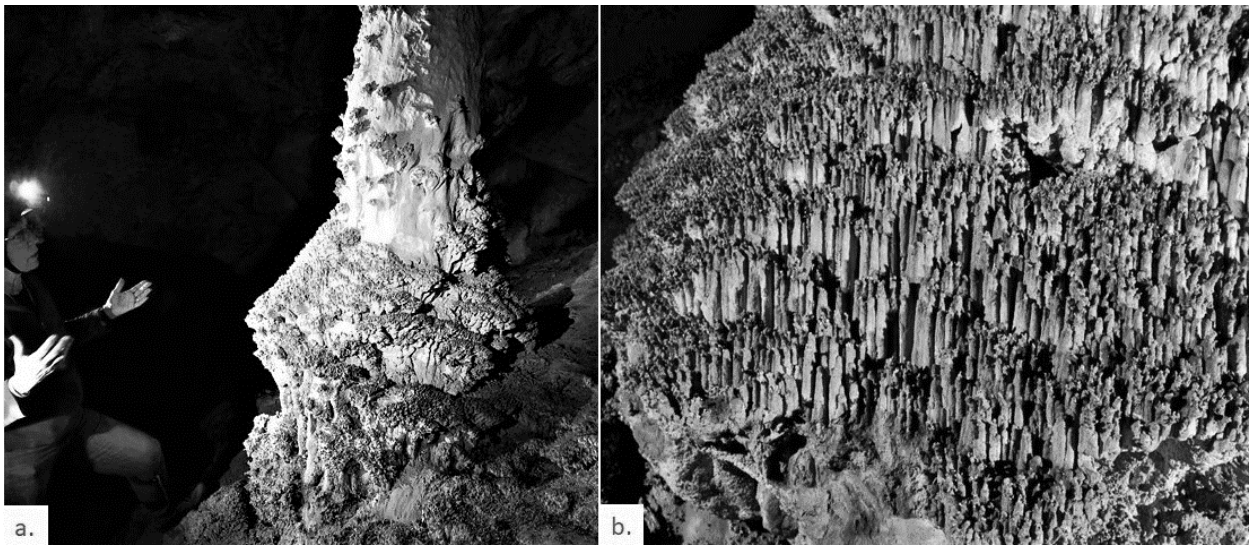

Figure 47